Plant Communications
Research Article

CellPress
PARTNER JOURNAL

BES1 Functions as the Co-regulator of D53-like SMXLs to Inhibit *BRC1* Expression in Strigolactone-Regulated Shoot Branching in *Arabidopsis*

Jie Hu[1], Yuanyuan Ji[1,2], Xiaotong Hu[1], Shiyong Sun[1,*] and Xuelu Wang[1,*]

[1]National Key Laboratory of Crop Genetic Improvement and Center of Integrative Biology, College of Life Science and Technology, Huazhong Agricultural University, Wuhan 430070, China

[2]Department of Genetics, School of Life Sciences, Fudan University, Shanghai 200438, China

***Correspondence: Shiyong Sun (sunshiyong@mail.hzau.edu.cn), Xuelu Wang (xlwang@mail.hzau.edu.cn)**

https://doi.org/10.1016/j.xplc.2019.100014

ABSTRACT

Shoot branching, determining plant architecture and crop yield, is critically controlled by strigolactones (SLs). However, how SLs inhibit shoot branching after its perception by the receptor complex remains largely obscure. In this study, using the transcriptomic and genetic analyss as well as biochemical studies, we reveal the key role of BES1 in the SL-regulated shoot branching. We demonstrate that BES1 and D53-like SMXLs, the substrates of SL receptor complex D14–MAX2, interact with each other to inhibit *BRC1* expression, which specifically triggers the SL-regulated transcriptional network in shoot branching. BES1 directly binds the *BRC1* promoter and recruits SMXLs to inhibit *BRC1* expression. Interestingly, despite being the shared component by SL and brassinosteroid (BR) signaling, BES1 gains signal specificity through different mechanisms in response to BR and SL signals.

Key words: strigolactones, shoot branching, signaling, D53-like SMXLs, BES1, BRC1

Hu J., Ji Y., Hu X., Sun S., and Wang X. (2020). BES1 Functions as the Co-regulator of D53-like SMXLs to Inhibit *BRC1* Expression in Strigolactone-Regulated Shoot Branching in *Arabidopsis*. Plant Comm. **1**, 100014.

INTRODUCTION

Strigolactones (SLs), a class of the terpenoid phytohormones (Gomez-Roldan et al., 2008; Umehara et al., 2008), are firstly recognized as symbiotic signals responsible for induction of seed germination of root parasite plants and as branching factors for symbiotic arbuscular mycorrhizal fungi (Cook et al., 1966; Akiyama et al., 2005). Although SLs have been recently found to regulate many plant developmental processes, including root hair elongation, primary root growth, adventitious and lateral root formation, secondary vascular growth, internode growth, and leaf senescence, inhibiting bud outgrowth in shoot branching regulation is one of their well-known functions in plants (Al-Babili and Bouwmeester, 2015). Mutants deficient in SL biosynthesis or signaling in *Arabidopsis thaliana* (*more axillary growth*, *max*), *Pisum sativum* (*ramosus*, *rms*), *Oryza sativa* (*dwarf*, *d*, or *high tillering dwarf*, *htd*), and *Petunia hybrida* (*decreased apical dominance*, *dad*), all exhibit enhanced branching phenotypes (Beveridge and Kyozuka, 2010; Domagalska and Leyser, 2011).

SL signaling is initiated when the α/β-hydrolase enzyme DWARF14 (D14) binds SLs and generates a covalently linked intermediate molecule. In turn, this triggers a conformational change in the structure of D14 to facilitate its interaction with an F-box protein DWARF3 (D3)/MAX2 (Nakamura et al., 2013; De Saint Germain et al., 2016; Yao et al., 2016). Recently, it was reported that D3 adopts a conformational state with a dislodged CTH (C-terminal α helix) to bind and inhibit D14 (Shabek et al., 2018). In an SL-dependent manner, D3/MAX2 induces the ubiquitination and degradation of its substrates to transduce SL signals, including D53/D53-like SMXLs (SUPPRESSOR OF MAX2-1 LIKEs, SMXL6, SMXL7, and SMXL8, three orthologs of D53 in *Arabidopsis* involved in shoot branching) (Jiang et al., 2013; Zhou et al., 2013; Soundappan et al., 2015; Wang et al., 2015), and a basic-helix-loop-helix transcription factor BES1 (*bri1*-EMS-SUPPRESSOR 1) (Wang et al., 2013). D53/D53-like SMXLs proteins, with ethylene-responsive element binding factor-associated amphiphilic repression (EAR) motifs, act as putative transcriptional

Published by the Plant Communications Shanghai Editorial Office in association with Cell Press, an imprint of Elsevier Inc., on behalf of CSPB and IPPE, CAS.

repressors to recruit TOPLESS-related proteins. Recently, the crystal structure study demonstrates that D53 promotes assembly of a corepressor–nucleosome complex with TPR2 through the EAR motif, which strongly suggests that the transcriptional regulation is key to transduce SL signaling (Ma et al., 2017). However, D53/D53-like SMXLs are transcription regulators without direct DNA-binding ability (Ma et al., 2017; Song et al., 2017), indicating that they need adaptors to affix DNA to mediate the SL-regulated transcription and shoot branching. BES1 is a transcription factor with DNA-binding activity that directly promotes or inhibits gene expression (Yin et al., 2005). Although BES1 is involved in the SL signaling by the D14–MAX2-mediated degradation in *Arabidopsis* (Wang et al., 2013), how BES1 mediates the transcriptional regulation in SL signaling is still unknown. In addition, the transcription factor *BRC1* (*BRANCHED 1*) has been reported to be a key switch for inhibiting shoot branching and is regulated by multiple environments and phytohormones, including SLs, in many plant species (Doebley et al., 1995; Aguilar-Martinez et al., 2007; Lewis et al., 2008; Martíntrillo et al., 2011; Choi et al., 2012; Dun et al., 2013; Gonzalez-Grandio et al., 2013). Although *BRC1* has been reported to regulate shoot branching genetically downstream of SL signaling (Aguilar-Martinez et al., 2007; Braun et al., 2012; Dun et al., 2012; Guan et al., 2012; Lu et al., 2013), the molecular mechanism of how SL signaling regulates *BRC1* is still unknown in *Arabidopsis*. It is known that transcriptional networks tightly orchestrate the growth and development of mammals and plants, and these networks are triggered by various developmental and environmental cues. Therefore, to complete a signaling pathway, key steps are to identify its essential transcription factors, and reveal that how those transcription factors are regulated by upstream signaling to trigger the signal-specific transcription networks (Hwang and Sheen, 2001; Valverde et al., 2004; Smit et al., 2005; Yin et al., 2005; Pinkston-Gosse and Kenyon, 2007). However, how SL signaling initiates the downstream transcriptional network after SL perception is still unknown.

In addition, BES1 has been initially identified as a primary signaling component in the brassinosteroid (BR) signaling pathway. It is tightly regulated mainly through the dynamic alteration of its phosphorylation status to transduce BR signal by the BR early signaling components, BIN2 (BRASSINOSTEROID INSENSITIVE 2) (Yin et al., 2002, 2005) and PP2A (PROTEIN PHOSPHATASE 2A) (Tang et al., 2011). In BR signaling, the non-phosphorylated and phosphorylated BES1s have different DNA-binding activities to regulate the BR-responsive genes (He et al., 2002). However, in the SL signaling pathway, both phosphorylated and non-phosphorylated BES1s are the direct substrates of SL receptor complex D14–MAX2 to control shoot branching (Wang et al., 2013). Interestingly, the BR signaling components upstream of BES1 display no function in shoot branching in *Arabidopsis* (Wang et al., 2013). This raises the question of how BES1 differentially functions in the BR and SL signaling to regulate signal-specific developmental processes.

Our transcriptomic and genetic analyss indicate that D53-like SMXLs and BES1 genetically depend on each other to regulate shoot branching through BRC1. This is further supported by the biochemical results thatBES1 physically interacts with D53-like SMXLs to inhibit *BRC1* expression, which depends on direct binding of BES1 to the *BRC1* promoter, and the EAR motif of D53-like SMXLs that represses the transcription of *BRC1*. In addition, we demonstrate that BRs treatment has no effect on the interaction of SMXLs with BES1 and the *BRC1* expression, and the altered phosphorylation status of BES1 cannot affect its DNA-binding ability with the *BRC1* promoter. Together, these findings reveal the mechanisms of how the BES1- D53-like SMXLs complexes transduce SL signals in shoot branching, and how BES1 differentially functions in SL and BR signaling pathways to control signal-specific developmental processes.

RESULTS

BES1- and *D53-like SMXLs* Genetically Depend on Each Other in Shoot Branching

To explore how SL signaling was involved in the transcriptional regulation in shoot branching, we detected the transcriptional profiles in the young buds (bud length $\leq$3 mm) of the SL signaling-related plant materials, including *MAX2:bes1-D-FLAG*/Columbia-0 (Col-0) (a gain-of-function form of *BES1*, which was stable under GR24-induced degradation, defined as *MAX2:bes1-D* below) (Wang et al., 2013), *SMXL7-D-GFP*/Col-0 (a gain-of-function form of genomic *SMXL7*, which was stable under GR24-induced degradation, defined as *SMXL7-D* below) (Jiang et al., 2013; Soundappan et al., 2015; Wang et al., 2015; Zhou et al., 2013), *Atd14-1*, and their wild-type Col-0. These materials were reported to exhibit the increased branching number compared with the wild-type Col-0 (Arite et al., 2009; Soundappan et al., 2015; Wang et al., 2013, 2015). First, 506 differentially expressed genes were identified from the comparison between *Atd14-1* and the wild-type Col-0, including 42 induced and 464 repressed genes (Supplemental Figure 1A and Supplemental Table 1). These genes were defined as SL-regulated genes because of the high specificity of the receptor AtD14 in SL signaling. There were 516 genes differentially expressed in buds from the comparison of *MAX2:bes1-D* versus the wild-type Col-0, including 15 upregulated and 501 downregulated genes (Supplemental Figure 1A and Supplemental Table 2). Significantly, 52.33% of the BES1-regulated genes were co-regulated by the SL receptor AtD14 (Figure 1A and Supplemental Figure 1A), and all of them were downregulated in both the *MAX2:bes1-D* and *Atd14-1* (Supplemental Figure 1B and Supplemental Table 3), suggesting that BES1 was a major transcription factor involved in the SL-regulated shoot branching. More independent *bes1-D* transgenic lines driven by the promoters of *MAX2* or *BES1*, and the *bes1-L-D* (BES1-L, the long form of BES1) (Jiang et al., 2015) transgenic lines driven by the 35S promoter further confirmed the function of BES1 in promoting shoot branching (Supplemental Figure 2A–2F). In addition, another published independent *BES1-RNAi* line with reduced expression of BES1 and its close homologs (Yin et al., 2005) also showed decreased branch number compared with the wild type (Supplemental Figure 2G and 2H). Furthermore, BES1 was highly expressed in the axillary buds as indicated by the *pBES1-L:GUS* and *pBES1-S:GUS* reporters (Supplemental Figure 3), supporting its key role in shoot branching. Second, there were 116 differentially expressed genes co-regulated by AtD14 and SMXL7 (Figure 1A, Supplemental Figure 1C, Supplemental Tables 4 and 5), all of which showed similar regulatory mode in the *Atd14-1* and *SMXL7-D* (Supplemental

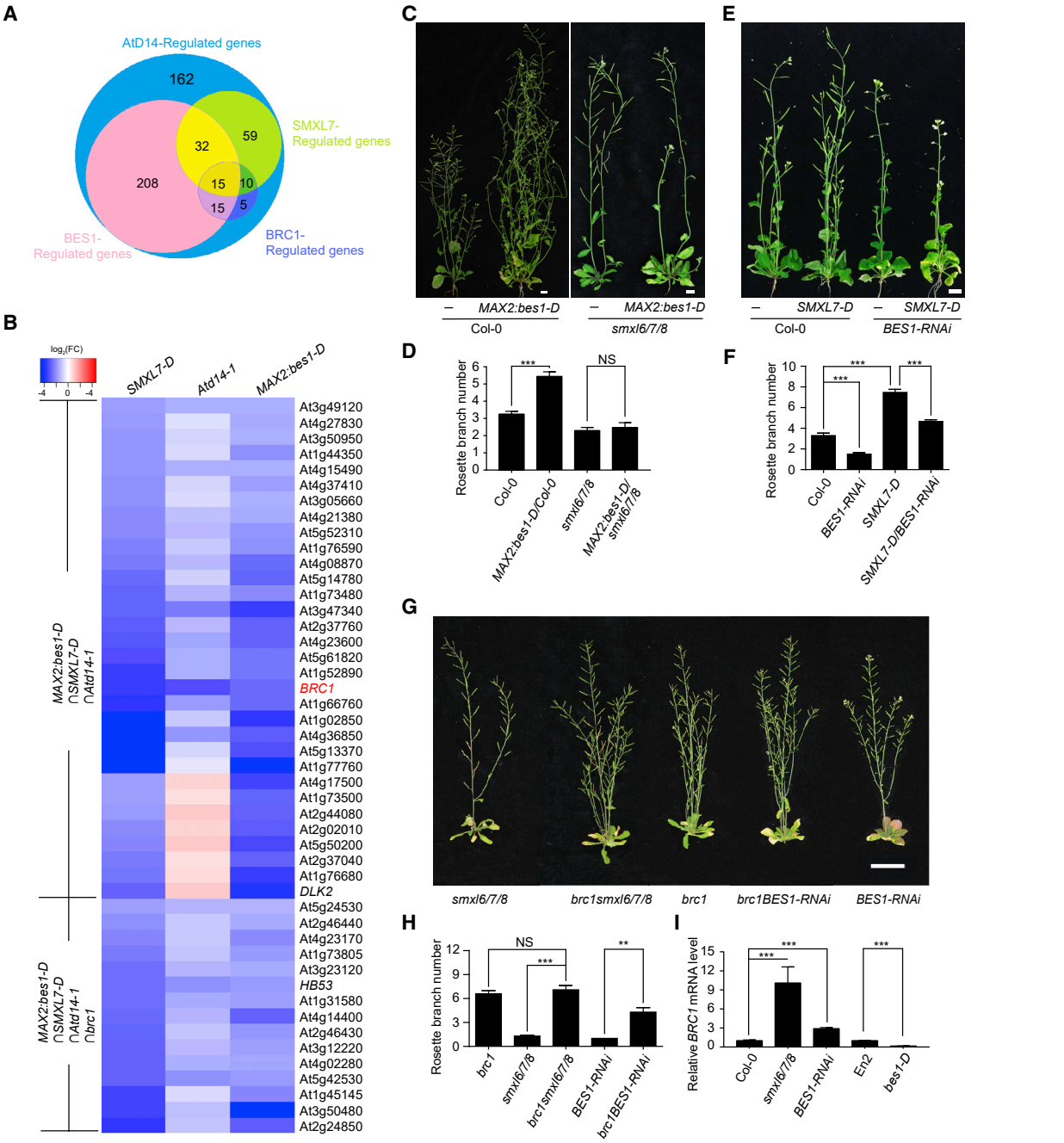

Figure 1. BES1- and D53-like SMXLs Genetically Depend on Each Other to Regulate BRC1-Mediated Shoot Branching through BRC1.

(A) Venn diagram of the number of differentially expressed genes in buds of *Atd14-1*, *SMXL7-D*, *MAX2:bes1-D*, and *brc1*, compared with Col-0, and co-regulated by AtD14. Differentially expressed genes in buds were obtained from cuffdiff analysis with q value <0.05.

(B) Heatmap of the 47 co-regulated genes by AtD14, SMXL7, and BES1 in **(A)**. Original fold change values were transformed by $\log_2$ regression for the heatmap shown in the colored bar.

(C) Phenotypes of Col-0, *MAX2:bes1-D*/Col-0, *smxl6/7/8*, and *MAX2:bes1-D/smxl6/7/8* plants. Scale bar corresponds to 1 cm.

(D) Quantification of rosette branch number of the plants in **(C)**. Data are means ± SE, Col-0 ($n = 20$), *MAX2:bes1-D*/Col-0 ($n = 27$), *smxl6/7/8* ($n = 27$), and *MAX2:bes1-Dsmxl6/7/8* ($n = 21$).

(E) Phenotypes of Col-0, *BES1-RNAi*, *SMXL7-D*, and *SMXL7-DBES1-RNAi* plants. Scale bar corresponds to 1 cm.

(F) Quantification of rosette branch number of the plants in **(E)**. Data are means ± SE, the sample number was Col-0 ($n = 17$), *BES1-RNAi* ($n = 26$), *SMXL7-D* ($n = 19$), and *SMXL7-DBES1-RNAi* ($n = 15$).

(G) Genetic analysis of BRC1, SMXLs, and BES1 in shoot branching. Scale bar corresponds to 5 cm.

(legend continued on next page)

Figure 1D). Significantly, 40.52% of them, 47 genes, were also regulated by BES1 (Figure 1A and 1B). Thus, we predicted that SMXL7 might be a major partner for the function of BES1 in SL-regulated shoot branching. Notably, there were still 223 genes co-regulated by BES1 and AtD14, but not by SMXL7 (Figure 1A), suggesting that BES1 was highly specific in the SL-regulated bud outgrowth, and that homologs of SMXL7 were also needed in SL signaling (Stanga et al., 2013, 2016; Wallner et al., 2017). Several key genes that have been reported to be involved in shoot branching were regulated by both BES1 and SMXL7 in the SL-regulated genes (Figure 1B). For example, *HB53* (*HOMEOBOX PROTEIN 53*), which encodes an HD-ZIP protein in axillary buds, inhibits shoot branching in response to abscisic acid (Gonzalez-Grandio et al., 2017). Importantly, the transcription factor *BRC1*, a key inhibitor for shoot branching (Aguilar-Martinez et al., 2007; Choi et al., 2012; Doebley et al., 1995; Dun et al., 2013; Gonzalez-Grandio et al., 2013; Lewis et al., 2008; Martíntrillo et al., 2011), was strongly co-regulated by BES1, SMXL7, and AtD14 (Figure 1B), which was consistent to its function in the downstream of SL signaling. Significantly, 53.57% of the BRC1-regulated genes were regulated by AtD14 (Figure 1A, Supplemental Figure 1A and Supplemental Table 6); and 89% of the genes co-regulated by BRC1 and AtD14 were regulated by BES1 and SMXL7 with similar regulatory modes in their buds (Figure 1B, Supplemental Figure 1E and 1F). Some genes that were reported to be involved in bud development, including *HB40* (*HOMEOBOX PROTEIN 40*), *NCED3* (*9-CIS-EPOXICAROTENOID. DIOXIGENASE 3*), *NAP* (*NAC-LIKE*, *ACTIVATED BY AP3/PI*), and *UGT74E2* (*UDP-glycosyltransferase 74E2*), were also found to be under BRC1 regulation (Figure 1B and Supplemental Figure 1E and 1F) (Dong et al., 2008; Tognetti et al., 2010; Gonzalez-Grandio et al., 2013, 2017; Holalu and Finlayson, 2017). Therefore, our transcriptome analysis suggests that the SL-regulated transcriptional network in shoot branching is largely dependent on the SMXLs–BES1–BRC1 module.

To further reveal the relationship among SMXLs, BES1, and BRC1 in SL-inhibited shoot branching, we performed a set of genetic analyses, and found that *MAX2:bes1-D* could not rescue the branching phenotype of the *smxl6/7/8* as indicated by the *MAX2:bes1-D/smxl6/7/8* line (Figure 1C and 1D), suggesting that BES1 required SMXLs to promote branching; similarly, the branch number of the *SMXL7-D/BES1-RNAi* was significantly decreased compared with the *SMXL7-D*/Col-0 line (Figure 1E and 1F), suggesting that SMXL7 also depended on BES1 to promote branching. Therefore, BES1- and D53-like SMXLs are likely dependent on each other to regulate shoot branching. Furthermore, *brc1* was able to rescue the branching phenotypes of either *smxl6/7/8* (Seale and Bennett, 2017) or the *BES1-RNAi* line (Figure 1G and 1H), which indicated that *BRC1* acted downstream of both *D53-like SMXLs* and *BES1* to control shoot branching. In addition, the *BRC1* expression was lower in the buds of *bes1-D*, *MAX2:bes1-D*/Col-0, and *SMXL7-D-GFP*/Col-0 lines, but higher in the *BES1-RNAi* lines, *smxl6/7/8* (Wang et al., 2015), the *MAX2:bes1-D-FLAG/smx6/7/8* lines, and the *SMXL7-D-GFP/BES1-RNAi* lines than in the wild type (Figure 1I and Supplemental Figure 4A–4C), indicating that knockdown of either BES1 or SMXLs could reduce the inhibitory effect on *BRC1* expression. Taken together, we conclude that the *D53-like SMXLs* and *BES1* genetically depend on each other to induce the SL-regulated transcriptional network mainly via *BRC1* for *Arabidopsis* shoot branching.

BES1 Interacts with D53-like SMXLs to Directly Inhibit *BRC1* Expression

Our further biochemical experiments demonstrated that SMXLs directly interacted with BES1 in pull-down assay, and also with BES1 and its homologs in bimolecular fluorescence complementation (BiFC) assays(Figure 2A and 2B and Supplemental Figure 5). In addition, both the phosphorylated and dephosphorylated BES1s were able to interact with SMXLs (Figure 2C), which was consistent with a previous report that both phosphorylated and dephosphorylated BES1s were able to interact with and be induced to be degraded by MAX2 (Wang et al., 2013), suggesting that both phosphorylated and dephosphorylated BES1s participated in SL signaling. Furthermore, BES1 interacted with D53-like SMXLs with or without additional SLs, BRs, or SLs plus BRs (Supplemental Figure 6).

D53/D53-like SMXLs have been reported to induce the oligomerization of TPL tetramer through linking tetramer–tetramer interaction and stabilize the TOPLESS corepressor–nucleosome interaction, which subsequently leads to the formation of repressive chromatin structures to inhibit transcription (Ke et al., 2015; Ma et al., 2017). Due to lacking direct DNA-binding ability, D53 requires an adaptor to specifically target promoters for transcriptional inhibition via chromatin modification (Ma et al., 2017; Song et al., 2017). Therefore, the interaction between BES1 and SMXLs raises the possibility that BES1 and its homologs likely serve as adaptors for SMXLs to proximate DNA and inhibit gene expression. To test this hypothesis, we detected whether BES1 could bind to the *BRC1* promoter. Chromatin immunoprecipitation (ChIP)-qPCR and electrophoretic mobility shift assay (EMSA) assays showed that BES1 directly bound to the *BRC1* promoter fragments F2, F4, and F5, which contain the E-box and GGTCC elements (BES1 binding cites reported in a previous study [Sun et al., 2010]) (Figure 3A–3C). Furthermore, to investigate the interdependency between BES1 and SMXLs to inhibit *BRC1* expression, we performed ChIP assays using the buds in the junction between shoots and roots of different plant materials (Supplemental Figure 7A). We detected the enrichment of *BRC1* promoter by SMXL7 in the buds of *SMXL7-D-GFP*/Col-0 and the *SMXL7-D-GFP/BES1-RNAi* lines using anti-GFP beads. The results showed the enrichment of *BRC1* promoter by SMXL7-D-GFP was much less in the *SMXL7-D-GFP/BES1-RNAi* plants than in the *SMXL7-D-GFP*/Col-0 plants

(H) Quantification of rosette branch number of the plants in **(G)**. Data are means ± SE, the sample number was *brc1* ($n = 20$), *smxl6/7/8* ($n = 20$), *brc1smxl6/7/8* ($n = 20$), *BES1-RNAi* ($n = 26$), and *brc1BES1-RNAi* ($n = 17$).

(I) Relative expression of *BRC1* in the buds of Col-0, *smxl6/7/8*, *BES1-RNAi*, En2, and *bes1-D* plants.

Data are means ± SD ($n = 6$) and P values in **(D)**, **(F)**, **(H)**, and **(I)** were determined by Student's t-test; $^{***}P < 0.001$, $^{**}P < 0.01$, non-significant (NS), $P > 0.05$. See also Supplemental Figures 1 and 2.

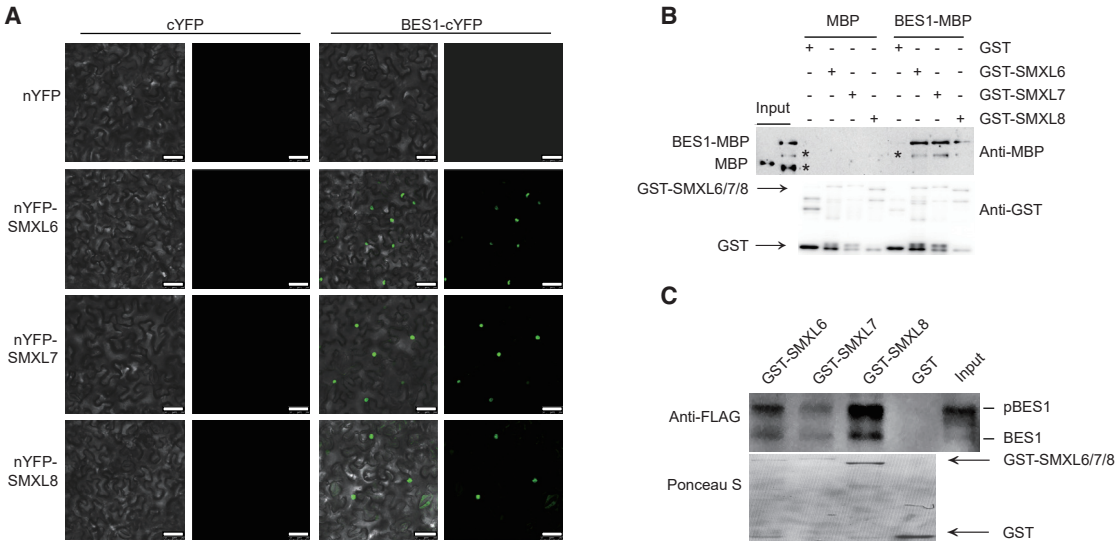

Figure 2. The D53-like SMXLs Interact with BES1.

(A) D53-like SMXLs interacted with BES1 in bimolecular fluorescence complementation assays. Scale bars correspond to 50 μm.

(B) D53-like SMXLs interacted with BES1 in a GST pull-down assay. Asterisks (*) indicated a nonspecific band. Anti-GST was used to show the amounts of the loaded GST and GST-SMXLs proteins.

(C) Both the phosphorylated and dephosphorylated forms of BES1 interacted with D53-like SMXLs in a semi-*in vivo* pull-down assay using *35S:BES1-FLAG* plants. Ponceau S staining showed the loaded GST and GST-SMXLs proteins.

See also Supplemental Figures 5 and 6.

(Figure 3D), resulting in a decreased inhibition of *BRC1* expression in buds of the *SMXL7-D-GFP/BES1-RNAi* line compared with that in the *SMXL7-D-GFP*/Col-0 line (Supplemental Figure 4B). It is indicated that the inhibition of SMXL7 on *BRC1* expression requires BES1 binding to the *BRC1* promoter. On the other hand, we detected the enrichment of the *BRC1* promoter by BES1 in buds of the *smxl6/7/8* and the Col-0 plants, and found that although the fragments of the *BRC1* promoter enriched by BES1 were significantly higher in the *smxl6/7/8* plant than in the Col-0 (Figure 3E), the *BRC1* expression level was still higher in the *smxl6/7/8* plant than that in Col-0 (Figure 1I and Supplemental Figure 4A), which meant that the inhibition of BES1 on *BRC1* expression required SMXLs. In addition, we also tested whether the interdependency between D53-like SMXLs and BES1 directly affected *BRC1* expression using the *BRC1:LUC* reporter in a transient expression assay in *N. benthamiana* leaves. The *SMXL7-D* and *bes1-D* were constructed as effectors, *35S:GFP* was used as the control effector, and *BRC1:LUC* linking *35S* controlling *Renilla* luciferase (*REN*) was the reporter (Figure 3F). The LUC/REN ratio was significantly reduced in *SMXL7-D/bes1-D* co-expressed lines compared with the lines expressing *SMXL7-D* or *bes1-D*, respectively (Figure 3G). We further measured the effect of D53-like SMXLs and BES1 on *BRC1* expression using a direct LUC reporter system in *N. benthamiana* leaves with *35S:LUC* as the reporter (Supplemental Figure 8A). The LUC intensity showed similar results that *BRC1* expression was largely inhibited by the co-expression of SMXLs and BES1 (Supplemental Figure 8B–8D). Therefore, the interdependency between BES1 and SMXL7 directly affects *BRC1* expression in shoot branching.

Because the transcriptional repression by the EAR-contained proteins was highly conserved and general in many signaling pathways among diverse plant species (Kagale and Rozwadowski, 2011), and that the EAR motif in SMXL7 was required for branching (Liang et al., 2016), we next asked whether the EAR motif in SMXL7 was also required by the BES1–SMXLs complex to inhibit *BRC1* expression. The *SMXL7-D-mEAR-GFP* was constructed to detect the function of the EAR motif of SMXL7 in regulating *BRC1* expression (Wang et al., 2015). We first tested and confirmed that *SMXL7-D-mEAR* showed a similar ability to interact with BES1 as SMXL7 and SMXL7-D (Supplemental Figure 9). When using either the dual bioluminescence or the *BRC1:LUC* reporter system in *N. benthamiana*, the activities of *BRC1:LUC* were significantly higher in the *SMXL7-D-mEAR/MAX2:bes1-D* than in the *SMXL7-D/MAX2:bes1-D* co-expressing leaves, and were significantly higher in the *SMXL7-D-mEAR* than in the *SMXL7-D* expressing leaves (Figure 3H and Supplemental Figure 8E–8G). To further investigate the function of the EAR motif of SMXL7 in shoot branching *in planta*, *SMXL7-D-GFP* and *SMXL7-D-mEAR-GFP* transgenic lines were generated. The *SMXL7-D-GFP* lines showed an increased number of rosette shoot branches, but the shoot branch number of the *SMXL7-D-mEAR-GFP* line was similar to that of the wild type (Supplemental Figure 7B and 7C), which was consistent with the results reported in a previous study (Liang et al., 2016). Furthermore, the transcription level of *BRC1* in the buds of the *SMXL7-D-mEAR-GFP* line showed no obvious difference from that of the wild type, but was remarkably higher than that in the *SMXL7-D-GFP* line (Supplemental Figure 7D). Therefore, the EAR motif of SMXLs is required by the SMXLs–BES1 complex to inhibit *BRC1* expression.

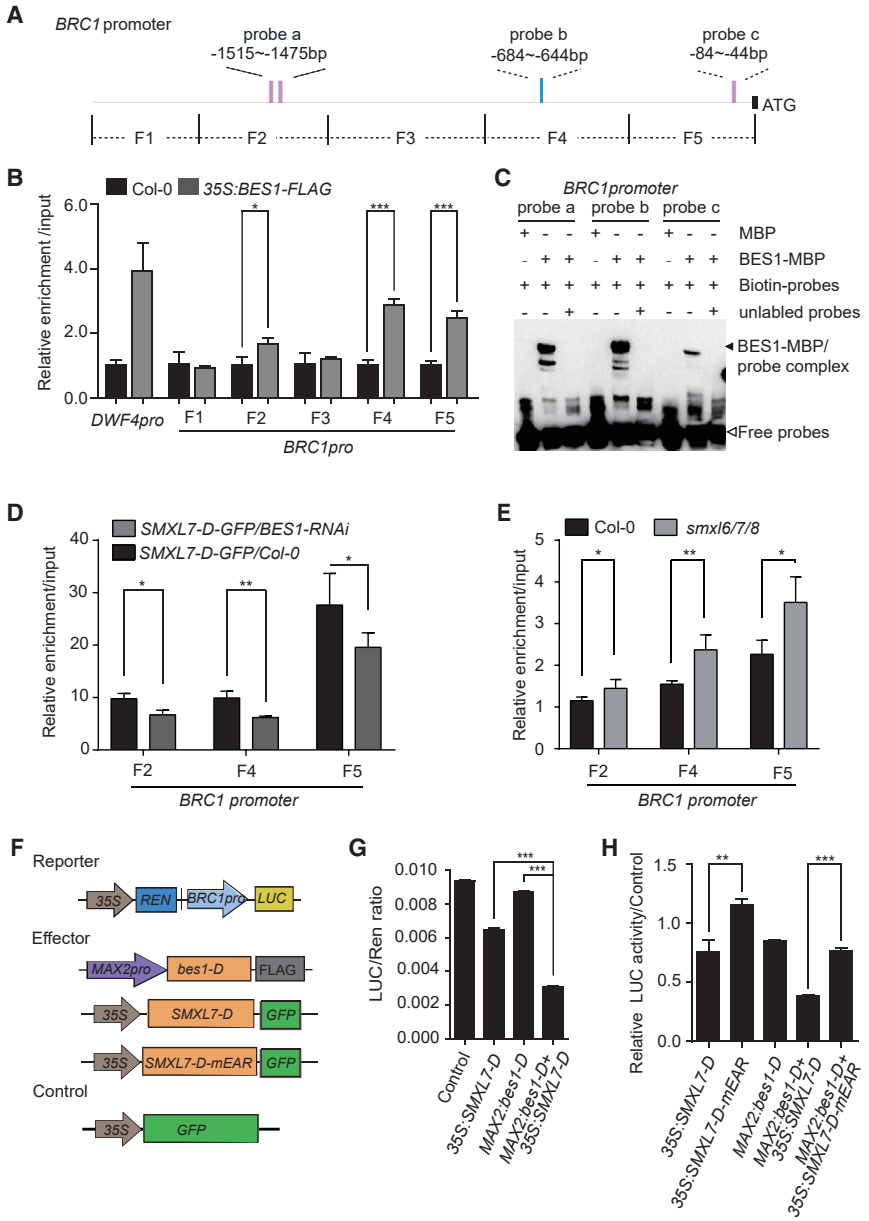

Figure 3. The D53-like SMXLs and BES1 Depend on Each Other to Directly Inhibit *BRC1* Expression in Shoot Branching.

(A) Schematic representation showed fragments and probes of the *BRC1* promoter in **(B)**–**(E)**. Pink bars indicated the *cis*-E-box. Blue bars show the GGTCC element.

(B and C) BES1-MBP directly bound to the *BRC1* promoter in ChIP–qPCR **(B)** and EMSA **(C)** assays. Solid and open triangles indicate BES1–MBP–DNA bands and free probe, respectively.

(D) The relative enrichment of *BRC1* promoter by SMXL7-GFP used anti-GFP beads in buds of *SMX7-D-GFP*/Col-0 and *SMX7-D-GFP/BES1-RNAi* plants.

(E) The relative enrichment of *BRC1* promoter used anti-BES1 antibody in buds of Col-0 and *smxl6/7/8* plants.

(F) Schematic diagrams of the luciferase reporter and effector constructs used in *N. benthamiana* transient assays.

(G) SMXL7 and BES1 corporately inhibited the expression of *BRC1:LUC*.

(H) Mutation of the EAR motif in SMXL7 reduced the inhibition of *BRC1* expression by the SMXLs–BES1 complex. LUC/REN ratio was normalized to the corresponding control defined as the relative LUC activity.

Data are means ± SD ($n = 3$) and P values in **(B)**–**(E)**, **(G)**, and **(H)** were determined by Student's t-test; $^{***}P < 0.001$, $^{**}P < 0.01$, $^{*}P < 0.05$.

See also Supplemental Figures 4, 7, 8, and 9.

BES1 Differentially Functions in SL and BR Signaling in *Arabidopsis*

Significantly, BES1 is differently regulated by SL and BR signaling in *Arabidopsis*. In BR signaling, BES1 is regulated through alteration of its phosphorylation status (Yang et al., 2017), the stability of BES1 is not primarily regulated by BR signaling in *Arabidopsis* (Jiang et al., 2015; Yang and Wang, 2017); while in SL signaling both the phosphorylated and dephosphorylated BES1s are induced to be degraded by MAX2 (Wang et al., 2013) and interact with D53-like SMXLs (Figure 2C and Supplemental Figure 6). Furthermore, mutants of the BR signaling components upstream of BES1 did not alter branch number (Wang et al., 2013) and *BRC1* expression (Figure 4A); and BR treatments had no effects on *BRC1* expression, while SLs effectively induced the *BRC1* expression with or without BRs (Figure 4B and Supplemental Figure 10). To further reveal the underlying reasons, we performed ChIP–qPCR assays using the BES1 antibody to detect the enrichment of *BRC1* promoter by BES1 in Col-0 and the BR receptor mutant *bril-301*, in which BES1 was mainly in phosphorylated status (Supplemental Figure 4D). Interestingly, BES1 in the BR receptor mutant *bril-301* had a similar ability to enrich the *BRC1* promoter, but had a largely reduced ability to enrich the *DWF4* promoter (Figure 4C), a well-known BR/BES1-targeted gene (He et al., 2005), which well explained the similar *BRC1* expression in the BR-related mutants and the wild type (Figure 4A), as well as the unchanged *BRC1* expression under BR treatments (Figure 4B). Taken together, these results demonstrate that the alteration of the BES1 phosphorylation status by BR signaling has no effect on *BRC1* expression and shoot branching, and that the function of BES1 in SL signaling is independent of that in BR signaling in *Arabidopsis* (Figure 4D). Therefore, when both SLs and BRs are present, BRs cannot change the SL-controlled shoot branching by altering the phosphorylated status of BES1 in *Arabidopsis* (Figure 4D).

DISCUSSION

In this study, we reveal that BES1 acts as the adaptor of D53-like SMXLs to trigger the SL-regulated transcriptional

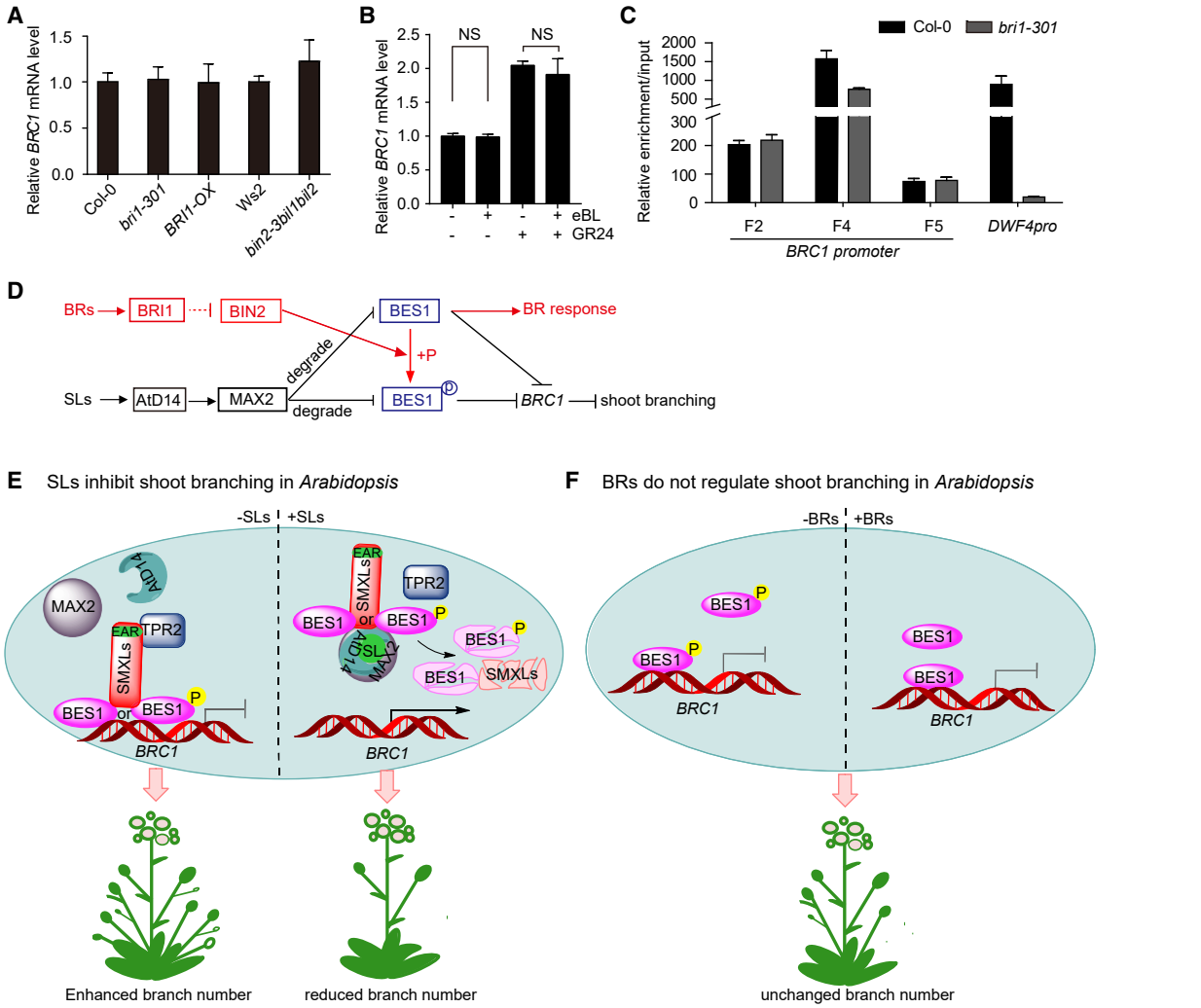

Figure 4. BES1 Functions Independently in SL and BR Signaling in *Arabidopsis*.

(A) Relative *BRC1* expression levels in the BR-related materials *bri301*, *BRI-OX*, and *bin2-3bil1bil2*.

(B) The transcription level of *BRC1* in isolated buds of Col-0 treated with mock, 5 μM eBL, 5 μM GR24, and 5 μM eBL plus 5 μM GR24 for 3 h, respectively.

(C) The ChIP–qPCR assays of the *BRC1* and *DWF4* promoters precipitated by BES1 in Col-0 and *bri1-301* plants using anti-BES1 antibody. Fold enrichment compared with the *ACTIN* promoter was normalized to their input.

(D) The model indicates that BES1 functions independently in SL and BR signaling in *Arabidopsis*. The alteration in the BES1 phosphorylation status by BR signaling has no effect on *BRC1* expression in shoot branching, while SL signaling regulates *BRC1* expression to inhibit shoot branching through degrading both phosphorylated and dephosphorylated BES1.

(E and F) Working models of the SL- and BR-mediated regulation of shoot branching in *Arabidopsis*. In *Arabidopsis*, when SLs are absent, D53-like SMXLs interact with phosphorylated or unphosphorylated BES1 to inhibit *BRC1* expression, via direct binding of BES1 to its promoter, and the EAR motif of D53-like SMXLs recruiting TPR2, leading to enhanced shoot branch number. When SLs are present, the D53-like SMXLs–BES1 complex is degraded by AtD14–MAX2 after SLs perception, resulting in the expression of *BRC1* to inhibit shoot branching **(E)**. In *Arabidopsis*, the phosphorylation status change caused by BRs has no effect on *BRC1* expression or shoot branching **(F)**.

Data are means ± SD (n = 3) and P values in **(B)** were determined by Student's t-test; non-significant (NS), $P > 0.05$.

See also Supplemental Figures 4 and 10.

network in the buds through the local transcription factor BRC1 for shoot branching in *Arabidopsis*. First, the genome-wide transcriptomes and genetic analysis using the SL signaling-related plant materials, suggest that BES1- and D53-like SMXLs interdependently trigger an SL-induced transcriptional network for shoot branching mainly through BRC1. Second, we demonstrate that BES1 interacts with D53-like SMXLs to inhibit *BRC1* expression, which is dependent on both the direct DNA binding by BES1 and the transcriptional inhibition by the EAR motif of D53-like SMXLs. Third, we reveal that BES1 functions independently in SL and BR signaling in *Arabidopsis.* Therefore, these data reveal a transcriptional regulation mechanism in the SL-controlled shoot branching via AtD14–MAX2–D53-like SMXLs–BES1–BRC1.

Our genetic and molecular results support the mechanism of how SL signaling directly inhibits *BRC1* expression to specifically inhibit bud outgrowth in *Arabidopsis.* In many

species, the TCP transcription factor *BRC1* and its homologs are proposed to be key switches to regulate bud outgrowth by coordinating diverse environmental and developmental cues (Doebley et al., 1995; Lewis et al., 2008; Martíntrillo et al., 2011; Dun et al., 2012; Gonzalez-Grandio et al., 2013; Mason et al., 2014; Holalu and Finlayson, 2017). However, the lack of a molecular mechanism by which *BRC1* regulates shoot branching means that it has long been controversial whether *BRC1* expression is necessary and sufficient for the inhibition of bud outgrowth (Seale and Bennett, 2017). A few studies support the important roles of BRC1 in SL-regulated shoot branching. For instance, the branching number of *brc1* is ascribed to rosette branching, but not cauline branching (Aguilar-Martinez et al., 2007), which is consistent with the branching phenotype of the SL-related mutants (Liang et al., 2016); and the expression of *BRC1* is also altered in the SL signaling mutants (Zhou et al., 2013; Chevalier et al., 2014; Wang et al., 2015). In addition, in pea and rice, *Psbrc1/Osfc1* mutants are insensitive to GR24 treatment and genetically function downstream of SL signaling to inhibit branching (or tillering in rice) (Aguilar-Martinez et al., 2007; Braun et al., 2012; Dun et al., 2012; Guan et al., 2012; Lu et al., 2013). In this study, first, our genetic and molecular results support that BES1 may directly control *BRC1* expression depending on D53-like SMXLs to promote bud outgrowth in *Arabidopsis* (Figure 1). Second, biochemical studies demonstrate that the D53-like SMXLs–BES1 module directly regulates *BRC1* expression via DNA binding by BES1 and transcriptional inhibition by the EAR motif of D53-like SMXLs (Figures 1 and 3 and Supplemental Figures 4, 7, and 8). Therefore, our study demonstrates that *BRC1*, as the SL signaling target, is directly regulated by BES1–SMXLs to inhibit bud outgrowth in *Arabidopsis.*

We also provide significant insights into how BES1, a component shared by SL and BR signaling pathways, differentially regulates signaling-specific biological processes in *Arabidopsis*. As a positive component in BR signaling and a key transcription factor directly regulating BR-responsive gene expression (Yin et al., 2005), BES1 regulates BR signaling outputs in *Arabidopsis* through switching between phosphorylated and dephosphorylated forms to alter its DNA binding and transcription activity (Yang and Wang, 2017; Yin et al., 2002). Recent studies demonstrate that the stability of BES1 is not primarily regulated by BR signaling in *Arabidopsis* (Jiang et al., 2015; Yang et al., 2017; Yang and Wang, 2017). While in the SL signaling pathway, both the phosphorylated and dephosphorylated forms of BES1 can interact with D53-like SMXLs (Figure 2), and can be induced to be degraded by MAX2 in response to SLs (Wang et al., 2013), indicating that the regulation of BES1 stability is a major mechanism in SL signaling. The differential regulation of BES1 by the two signals indicates that BES1 independently functions in the BR and SL signaling pathways to control different development processes in *Arabidopsis* (Figure 4D). Consistent with this hypothesis, mutants of the BR signaling components upstream of BES1 have similar branching number (Wang et al., 2013) and similar expression level of *BRC1* (Figure 4A) compared with wild type in *Arabidopsis*; and BR treatment has no effect on *BRC1* expression in buds and on the interaction between BES1- and D53-like SMXLs (Figure 4B and Supplemental Figure 6). Furthermore, the altered phosphorylation status of BES1 cannot affect its ability binding to the *BRC1* promoter (Figure 4C). These results all support the conclusion that BES1 independently functions in SL and BR signaling to trigger the signal-specific gene expression (Figure 4D).

In addition, a number of genetic data strengthen our conclusion that BES1 and its homologs play an important role in regulating shoot branching in *Arabidopsis*. In *Arabidopsis*, BES1 has five homologous genes, BZR1 and BEH1-4. BES1 and its homologs have been reported to work redundantly in BR signaling (Chen et al., 2019; Yin et al., 2005). In addition, it is also known that the homologous genes of *BES1* in *Arabidopsis* are redundant in SL signaling, because *BES1* and its homologs are able to interact with MAX2 (Wang et al., 2013) and the D53-like SMXLs (Figure 2 and Supplemental Figure 5). Thus, the *BES1-RNAi* line, with the reduced expression of *BES1* and its homologous genes, displays reduced rosette branching number (Wang et al., 2013) (Figure 1E and 1F and Supplemental Figure 2), and suppresses the branching phenotype of *max2-1* (Wang et al., 2013), which well explained why a T-DNA-insertion line, *bes1-1*, which has abolishes BES1 expression, exhibiting a slightly reduced rosette branches and similar cauline branches compared with that in Col-0 (Bennett et al., 2016). In addition, the *bes1-D* mutant line in En2 background and the transgenic lines, by expressing *bes1-D* in the Col-0 background, all exhibited the BR-enhanced phenotypes similar to plants overproducing BRs or *BRI1* (Yin et al., 2002), also presented the more branching number than wild-type control in *Arabidopsis* (Figure 1C, Supplemental Figure 2 and Wang et al., 2013). In this study, the branching phenotype of more independent transgenic lines, including *bes1-D* and *BES1-RNAi* (Supplemental Figure 2) further supported the function of BES1 in shoot branching. In addition, in a parallel study, we demonstrated that the *OsBZR1-RNAi* line (the homolog of *BES1* in rice) also exhibits the reduced tiller number, and rescues the tillering phenotype of *d14*, *d3*, and *d53* in rice; we also demonstrated that the *OsBZR1:Osbzr1-D* transgenic rice had more tillers than the wild-type Nipponbare. Taken together, these results suggest that the function of *AtBES1/OsBZR1* in shoot branching is general and conserved in *Arabidopsis* and rice.

Therefore, we propose a molecular mechanism how the SL signal is transduced to trigger the transcriptional network in *Arabidopsis* buds (Figure 4E and 4F). When SLs are insufficient, D53-like SMXLs and BES1, the direct substrates of D14–MAX2, are accumulated, and interact with each other to bind the *BRC1* promoter via BES1, which inhibits *BRC1* expression by the EAR motif of D53-like SMXLs to increase shoot branching; when SLs are sufficient, BES1 and D53-like SMXLs are all ubiquitinated and induced to be degraded by AtD14–MAX2 complex in buds, which relieves the inhibition of *BRC1* expression to inhibit bud outgrowth (Figure 4E). Whereas, the alteration between phosphorylated and dephosphorylated BES1s induced by BR signaling has no effect on the *BRC1*expression, and does not change the branch number in *Arabidopsis* (Figure 4F). Therefore, multiple mechanisms have been evolved in regulating BES1 for

decoding distinct developmental and environmental cues in plants.

METHODS

Plant Materials

The *Arabidopsis thaliana* mutant alleles used in this study were: *brc1* (*SALK_091920C*) (Aguilar-Martinez et al., 2007), *BES-RNAi* (Yin et al., 2005), *smxl6* (*CS847925/SAIL_1285_H05*), *smxl7* (*SALK_082032*), *smxl8* (*SALK_126406*) (described in Wang et al., 2015), *Atd14-1* mutant (isolated from the Wisconsin DsLox T-DNA insertion collection [*CS913109* (*N913109*)]) (Waters et al., 2012; Vegh et al., 2017), and *max2-1* (SALK_092836). All were in the Col-0 background, as well as the *brc1smxl6/7/8*, *brc1BES1-RNAi* mutants, and the 35S:*BES1-FLAG*, *SMXL7-D-GFP*, *SMXL7-D-GFPBES1-RNAi*, *SMXL7-D-mEAR-GFP*, and *MAX2:bes1-D smxl6/7/8* transgenic plants. Surface-sterilized seeds were sown on 0.8% agar plates containing Murashige and Skoog (MS) medium. Plates were kept in darkness for 2–3days, and then placed at 22°C under light conditions (16-h light/8-h dark long-day). Primers used for genotyping of these mutants were listed in Supplemental Table 7.

Construction of Transgenic Lines

The *Arabidopsis* quadruple mutant *brc1smxl6/7/8* was generated from a cross between homozygous *brc1* and the triple mutant *smxl6/7/8*, and identified from F2 lines. *brc1BES1-RNAi* was also obtained from their F2 progeny. Genotyping of the *brc1*, *smxl6*, *smxl7*, and *smxl8* mutants was performed by PCR. For *Arabidopsis*, constructs used to generate transgenic plants were *pCAMBIA* 1300 with different tags, including *SMXL7-D-GFP*, *SMXL7-D-GFP*, *SMXL7-D-mEAR-GFP*, and *MAX2:bes1-D.* The genomic DNA fragment of *SMXL7*, including the promoter region and the transcription region without the stop codon by overlapping PCR (using primer SMXL7pro and SMXL7-R listed in Supplemental Table 7), was fused in-frame to the 5′ end of *GFP*. *SMXL7-D* was constructed by overlapping PCR (using primer overlapping-SMXL7-D-F2/R2 listed in Supplemental Table 7) according to the 15-bp deletion of D53 in rice and SMXL7 in *Arabidopsis*, and resulted in substitution of the amino acids RGKTGI with a single threonine residue (Jiang et al., 2013; Soundappan et al., 2015; Wang et al., 2015; Zhou et al., 2013), which was also fused to the 5′ end of *GFP* with its promoter. *SMXL7-D-mEAR* was constructed based on plasmid *SMXL7-D* by overlapping PCR (using primer overlapping-SMXL7-mEAR-F2/R2 listed in Supplemental Table 7) according to the previous study (Liang et al., 2016). BES1 was amplified using primer BES1-F/R (Supplemental Table 7) to constructed *MAX2:bes1-D-FLAG* and *35S-BES1-cYFP*, and primer BES1-L-F/BES1-R (Supplemental Table 7) to construct 35S:BES1-L-D-mCherry. Genomic BES1 was amplified using BES1pro-F and BES1-R (Supplemental Table 7). Mutated-form *bes1-D* was obtained by overlapping PCR (using primer overlapping-bes1-D-F/R listed in Supplemental Table 7) according to a previous study (Yin et al., 2002). *pBES1-L:GUS* and *pBES1-S:GUS* transgenic lines were used in this paper (Jiang et al., 2015). Constructs were then transfected into Col-0, *BES1-RNAi*, or *smxl6/7/8* by agroinfiltration using the floral dip method (Clough and Bent, 1998). T_3 homozygous lines were generated and analyzed for each construct. Primers are listed in Supplemental Table 7.

BiFC, LUC Reporter Assay, and Dual Bioluminescence Assay

For BiFC assays, the full-length coding sequence of each *D53-like SMXLs*, fused with N-terminal *YFP*, was cloned into *PXY106* vectors. *BES1* and its homologous genes, fused with C-terminal *YFP*, were constructed into *PXY104* using the Seamless cloning/in-fusion cloning system. For the LUC reporter assay, the *BRC1* promoter (2067 bp length upstream from ATG) and its first exon was constructed into *pCAMBIA*1300, with *LUC* as the reporter, and *35S* promoter-linked *LUC* genes as the control reporter. For the effector SMXL7-D, SMXL7-mEAR was constructed into *pCAMBIA1300* under the control of a *35S* promoter and fused to the 5′ end of the *GFP* gene, mutated-form SMXL7-D and SMXL7-D-mEAR were constructed as above (described in part construction of transgenic lines), based on the coding sequence of SMXL7 which was amplified using primer SMXL7-F/R (Supplemental Table 7). *MAX2:bes1-D* was same as the plasmid used to construct the transgenic plant *MAX2:bes1-D-FLAG*/Col-0. Empty plasmid *pCAMBIA1300* with *GFP* genes under a *35S* promoter was used as the control effector.

For dual bioluminescence assays, the *BRC1* promoter (2067 bp length with ATG) controlling the *LUC* reporter gene was constructed into *pGreenII 0800-LUC*, linked to a *35S* promoter regulating the *renilla* (*REN*) reporter gene, which was used as the reference. The effectors *35S:SMXL7-D-GFP*, *35S:SMXL7-mEAR-GFP*, and *MAX2:bes1-D-FLAG* were constructed in the same way as in the LUC reporter assay. Primers are listed in Supplemental Table 7. *Agrobacterium* strain GV3101 was transformed with the above vector, then injected into young leaves of *N. benthamiana*. Plants were grown in the dark for 1 day, then transferred to long-day conditions (16 h light/8 h dark) for 2 days. Fluorescence signals in pavement cells were observed with confocal microscopy (Leica SP8). For the luciferase reporter assay, 2 mM luciferin was used to observe the fluorescence using a CCD system (LUMAZONE PYLON2048B). For dual bioluminescence assay, the fluorescence of LUC and REN were detected using the Dual-Luciferase Report Assay System by Mithras LB940.

In Vitro Pull-Down Assay

The coding sequence of each gene in the *D53-like SMXLs* family was cloned into *pGEX-4T-1* to obtain GST-SMXLs recombinant proteins. Primers are listed in Supplemental Table 7. GST fusion proteins and MBP fusion proteins were purified using glutathione beads (GenScript), and amylose resin (NEB), respectively. Glutathione beads containing GST or GST-SMXLs were incubated with MBP, MBP-BES1 in 1× PBS at 4°C for 2 h. Beads were washed 8–10 times with wash buffer (1× PBS, 0.1% Triton X-100) and boiled with 1× SDS loading buffer at 95°C for 5–10 min, separated by SDS–PAGE, and immunoblotted with anti-MBP antibodies (produced in our lab by rabbits immunized with full-length MBP protein).

Semi-*in Vivo* Pull-Down Assay

Semi-*in vivo* pull-down assays were performed using *35S:BES1-FLAG* transgenic plants, which were grown on $^1/_2$ MS medium for 15 days. Plant materials were ground to powder in liquid nitrogen and solubilized with 2× protein extraction buffer (100 mM Tris–HCl [pH 7.5], 300 mM NaCl, 2 mM EDTA [pH 8.0], 1% Triton X-100, 10% glycerol, and protease inhibitor). Extracts were centrifuged twice at 12 000 rpm for 10 min, and the resulting supernatants were collected and incubated with either GST or GST-SMXLs pre-incubated GST beads at 4°C for 2 h. Beads were washed about five times with wash buffer, and then boiled with 1× SDS loading buffer at 95°C for 5–10 min, separated by SDS–PAGE, and immunoblotted with anti-FLAG antibodies.

RT–PCR and RNA Sequencing

Rosette buds ≤3 mm were excised from different plants, which were about 5–10 cm high with only one main branch. Excised buds were immediately put into liquid nitrogen, then collected for RNA extraction. Total RNA was prepared using a plant total RNA extraction kit (TIANGEN), according to the users' manual. For qRT–PCR, RNA samples were reverse transcribed using a first-strand cDNA synthesize kit (Takara) and oligo(dT). Real-time PCR experiments were performed using gene-specific primers (Supplemental Table 7) on a CFX 96 real-time PCR detection system (Bio-Rad) in a total volume of 10 μl containing 2 μl diluted cDNA, 0.3 mM gene-specific primers, and 5 μl SYBR Green Supermix (Bio-Rad). The *Arabidopsis U-box* gene was used as the internal control. RNA samples were sent to the Beijing Genomics Institute for RNA sequencing (RNA-seq). The RNA-seq data that support the findings of this study are available.

ChIP

Using the method published by Fiil et al. (2008), Col-0 and *BES1-FLAG* seedlings of about 2–3-weeks-old or buds with junction of shoot and root of Col-0, *smxl6/7/8*, *SMXL7-D-GFP*/Col-0, and *SMXL7-D-GFP*/*BES1-RNAi* lines were harvested with Fix Buffer (0.4 M sucrose, 10 mM Tris–HCl [pH 8.0], 1 mM EDTA, 1 mM PMSF, 1.0% formaldehyde). Seedlings were vacuum-infiltrated for 30 min for crosslinking. Anti-FLAG gels, anti-GFP gels (40 μl) or endogenous anti-BES1 antibody (needed to preclear the chromatin sample using 100–200 μl protein A resin) was used for immunoprecipitation of BES1–DNA complex. Regarding anti-FLAG and anti-GFP gels, chromatin was incubated with gels at 4°C overnight using a rotating mixer wheel before collected. While, as for anti-AtBES1 antibody, after being rotated at 4°C overnight, 40 μl of protein A resin was added and rotated at 4°C for 3 h to collected the BES1–DNA complex. Finally, DNA was isolated by phenol:chloroform. Finally, 50 μl of Milli-Q water was added to dissolve the pellet DNA.

EMSA

The amplified coding sequences of *BES1* were fused in-frame with *MBP* tags and transformed into *Escherichia coli*. BES1-MBP recombinant proteins were purified. MBP was purified as the control. Recombinant proteins were then incubated with biotin-labeled probes, or with corresponding unlabeled probes for 30 min in EMSA-binding buffer (Thermo Fisher Scientific). Reaction mixtures were separated by non-denaturing polyacrylamide. DNA signals were detected by chemiluminescence.

Quantification and Statistical Analysis

qRT–PCR data were collected using Bio-Rad real-time PCR detection systems. These data were assumed to follow normal distributions and were subjected to one-tailed or two-tailed Student's *t*-tests according to F-test results. Statistical tests were performed in Microsoft Excel 2016. Statistical parameters, including the exact value of *n*, the precision measures (mean ± SD) or (mean ± SE) and statistical significance, can be found in the figure legends. Here, *n* means number of plants for phenotypic analysis, or numbers of technical replicates for qRT–PCR. In Figures, asterisks denote statistical significance test (***$P < 0.001$, **$P < 0.01$, *$P < 0.05$, non-significant [NS], $P > 0.05$) compared with the corresponding controls, unless otherwise specified by lines connecting the compared pieces of data.

SUPPLEMENTAL INFORMATION

Supplemental Information is available at *Plant Communications Online*.

FUNDING

Supported by NSFC 31430046 (to X.W), 31661143024 (to X.W.), National Key Research and Development Plan 2016YFD0100403 (to S.S.), the Ministry of Agriculture Innovation team plan (0120150092 to X.W.), the School Independent Scientific and Technological Innovation Foundation and Research Startup Foundation of Huazhong Agricultural University (2662015PY020 and 2014RC002 to X.W.).

AUTHOR CONTRIBUTIONS

X.W., S.S., and J.H. designed the experiments and wrote the manuscript. J.H., Y.J., and X.H. performed the experiments and analyzed the data.

ACKNOWLEDGMENTS

We thank J.Y. Li (Institute of Genetics and Developmental Biology, Chinese Academy of Sciences) for providing the mutants *smxl6/7/8*. No conflict of interest declared.

Received: November 1, 2019
Revised: December 5, 2019
Accepted: December 8, 2019
Published: December 12, 2019

REFERENCES

Aguilar-Martinez, J.A., Poza-Carrion, C., and Cubas, P. (2007). *Arabidopsis* BRANCHED1 acts as an integrator of branching signals within axillary buds. Plant Cell **19**:458–472.

Akiyama, K., Matsuzaki, K., and Hayashi, H. (2005). Plant sesquiterpenes induce hyphal branching in arbuscular mycorrhizal fungi. Nature **435**:824–827.

Al-Babili, S., and Bouwmeester, H.J. (2015). Strigolactones, a novel carotenoid-derived plant hormone. Annu. Rev. Plant Biol. **66**:161–186.

Arite, T., Umehara, M., Ishikawa, S., Hanada, A., Maekawa, M., Yamaguchi, S., and Kyozuka, J. (2009). d14, a strigolactone-insensitive mutant of rice, shows an accelerated outgrowth of tillers. Plant Cell Physiol. **50**:1416–1424.

Bennett, T., Liang, Y., Seale, M., Ward, S., Muller, D., and Leyser, O. (2016). Strigolactone regulates shoot development through a core signalling pathway. Biol. Open **5**:1806–1820.

Beveridge, C.A., and Kyozuka, J. (2010). New genes in the strigolactone-related shoot branching pathway. Curr. Opin. Plant Biol. **13**:34–39.

Braun, N., de Saint Germain, A., Pillot, J.P., Boutet-Mercey, S., Dalmais, M., Antoniadi, I., Li, X., Maia-Grondard, A., Le Signor, C., Bouteiller, N., et al. (2012). The pea TCP transcription factor PsBRC1 acts downstream of strigolactones to control shoot branching. Plant Physiol. **158**:225–238.

Chen, L.-G., Gao, Z., Zhao, Z., et al. (2019). BZR1 family transcription factors function redundantly and indispensably in BR signaling but exhibit BRI1-independent function in regulating anther development in Arabidopsis. Mol. Plant **12**:1408–1415.

Chevalier, F., Nieminen, K., Sanchez-Ferrero, J.C., Rodriguez, M.L., Chagoyen, M., Hardtke, C.S., and Cubas, P. (2014). Strigolactone promotes degradation of DWARF14, an alpha/beta hydrolase essential for strigolactone signaling in *Arabidopsis*. Plant Cell **26**:1134–1150.

Choi, M.S., Woo, M.O., Koh, E.B., Lee, J., Ham, T.H., Seo, H.S., and Koh, H.J. (2012). Teosinte Branched 1 modulates tillering in rice plants. Plant Cell Rep. **31**:57–65.

Clough, S.J., and Bent, A.F. (1998). Floral dip: a simplified method for *Agrobacterium*-mediated transformation of *Arabidopsis thaliana*. Plant J. **16**:735–743.

Cook, C.E., Whichard, L.P., Turner, B., Wall, M.E., and Egley, G.H. (1966). Germination of witchweed (*Striga lutea* Lour.): isolation and properties of a potent stimulant. Science **154**:1189–1190.

De Saint Germain, A., Clave, G., Badet-Denisot, M.A., Pillot, J.P., Cornu, D., Le Caer, J.P., Burger, M., Pelissier, F., Retailleau, P., Turnbull, C., et al. (2016). An histidine covalent receptor and butenolide complex mediates strigolactone perception. Nat. Chem. Biol. **12**:787–794.

Doebley, J., Stec, A., and Gustus, C. (1995). *teosinte* branched1 and the origin of maize: evidence for epistasis and the evolution of dominance. Genetics **141**:333–346.

Domagalska, M.A., and Leyser, O. (2011). Signal integration in the control of shoot branching. Nat. Rev. Mol. Cell Biol. **12**:211–221.

Dong, G., Ma, D.P., and Li, J. (2008). The histone methyltransferase SDG8 regulates shoot branching in *Arabidopsis*. Biochem. Biophys. Res. Commun. **373**:659–664.

Dun, E.A., de Saint Germain, A., Rameau, C., and Beveridge, C.A. (2012). Antagonistic action of strigolactone and cytokinin in bud outgrowth control. Plant Physiol. **158**:487–498.

Dun, E.A., de Saint Germain, A., Rameau, C., and Beveridge, C.A. (2013). Dynamics of strigolactone function and shoot branching responses in Pisum sativum. Mol. Plant **6**:128–140.

Fiil, B.K., Qiu, J.L., Petersen, K., Petersen, M., and Mundy, J. (2008). Coimmunoprecipitation (co-IP) of nuclear proteins and chromatin immunoprecipitation (ChIP) from *Arabidopsis*. CSH Protoc. **2008**. https://doi.org/10.1101/pdb.prot5049.

Gomez-Roldan, V., Fermas, S., Brewer, P.B., Puech-Pages, V., Dun, E.A., Pillot, J.P., Letisse, F., Matusova, R., Danoun, S., Portais, J.C., et al. (2008). Strigolactone inhibition of shoot branching. Nature **455**:189–194.

Gonzalez-Grandio, E., Poza-Carrion, C., Sorzano, C.O., and Cubas, P. (2013). BRANCHED1 promotes axillary bud dormancy in response to shade in *Arabidopsis*. Plant Cell **25**:834–850.

Gonzalez-Grandio, E., Pajoro, A., Franco-Zorrilla, J.M., Tarancon, C., Immink, R.G., and Cubas, P. (2017). Abscisic acid signaling is controlled by a BRANCHED1/HD-ZIP I cascade in *Arabidopsis* axillary buds. Proc. Natl. Acad. Sci. U S A **114**:E245–E254.

Guan, J.C., Koch, K.E., Suzuki, M., Wu, S., Latshaw, S., Petruff, T., Goulet, C., Klee, H.J., and McCarty, D.R. (2012). Diverse roles of strigolactone signaling in maize architecture and the uncoupling of a branching-specific subnetwork. Plant Physiol. **160**:1303–1317.

He, J.X., Gendron, J.M., Yang, Y., Li, J., and Wang, Z.Y. (2002). The GSK3-like kinase BIN2 phosphorylates and destabilizes BZR1, a positive regulator of the brassinosteroid signaling pathway in *Arabidopsis*. Proc. Natl. Acad. Sci. U S A **99**:10185–10190.

He, J.X., Gendron, J.M., Sun, Y., Gampala, S.S., Gendron, N., Sun, C.Q., and Wang, Z.Y. (2005). BZR1 is a transcriptional repressor with dual roles in brassinosteroid homeostasis and growth responses. Science **307**:1634–1638.

Holalu, S.V., and Finlayson, S.A. (2017). The ratio of red light to far red light alters *Arabidopsis* axillary bud growth and abscisic acid signalling before stem auxin changes. J. Exp. Bot. **68**:943–952.

Hwang, I., and Sheen, J. (2001). Two-component circuitry in *Arabidopsis* cytokinin signal transduction. Nature **413**:383–389.

Jiang, L., Liu, X., Xiong, G., Liu, H., Chen, F., Wang, L., Meng, X., Liu, G., Yu, H., Yuan, Y., et al. (2013). DWARF 53 acts as a repressor of strigolactone signalling in rice. Nature **504**:401–405.

Jiang, J., Zhang, C., and Wang, X. (2015). A recently evolved isoform of the transcription factor BES1 promotes brassinosteroid signaling and development in *Arabidopsis thaliana*. Plant Cell **27**:361–374.

Kagale, S., and Rozwadowski, K. (2011). EAR motif-mediated transcriptional repression in plants: an underlying mechanism for epigenetic regulation of gene expression. Epigenetics **6**:141–146.

Ke, J., Ma, H., Gu, X., Thelen, A., Brunzelle, J.S., Li, J., Xu, H.E., and Melcher, K. (2015). Structural basis for recognition of diverse transcriptional repressors by the TOPLESS family of corepressors. Sci. Adv. **1**:e1500107.

Lewis, J.M., Mackintosh, C.A., Shin, S., Gilding, E., Kravchenko, S., Baldridge, G., Zeyen, R., and Muehlbauer, G.J. (2008). Overexpression of the maize Teosinte Branched1 gene in wheat suppresses tiller development. Plant Cell Rep. **27**:1217–1225.

Liang, Y., Ward, S., Li, P., Bennett, T., and Leyser, O. (2016). SMAX1-LIKE7 signals from the nucleus to regulate shoot development in *Arabidopsis* via partially EAR motif-independent mechanisms. Plant Cell **28**:1581–1601.

Lu, Z., Yu, H., Xiong, G., Wang, J., Jiao, Y., Liu, G., Jing, Y., Meng, X., Hu, X., Qian, Q., et al. (2013). Genome-wide binding analysis of the transcription activator ideal plant architecture1 reveals a complex network regulating rice plant architecture. Plant Cell **25**:3743–3759.

Ma, H., Duan, J., Ke, J., He, Y., Gu, X., Xu, T.H., Yu, H., Wang, Y., Brunzelle, J.S., and Jiang, Y. (2017). A D53 repression motif induces oligomerization of TOPLESS corepressors and promotes assembly of a corepressor-nucleosome complex. Sci. Adv. **3**. https://doi.org/10.1126/sciadv.1601217.

Martíntrillo, M., Grandío, E.G., Serra, F., Marcel, F., Rodríguezbuey, M.L., Schmitz, G., Theres, K., Bendahmane, A., Dopazo, H., and Cubas, P. (2011). Role of tomato BRANCHED1-like genes in the control of shoot branching. Plant J. **67**:701–714.

Mason, M.G., Ross, J.J., Babst, B.A., Wienclaw, B.N., and Beveridge, C.A. (2014). Sugar demand, not auxin, is the initial regulator of apical dominance. Proc. Natl. Acad. Sci. U S A **111**:6092–6097.

Nakamura, H., Xue, Y.L., Miyakawa, T., Hou, F., Qin, H.M., Fukui, K., Shi, X., Ito, E., Ito, S., and Park, S.H. (2013). Molecular mechanism of strigolactone perception by DWARF14. Nat. Commun. **4**:2613.

Pinkston-Gosse, J., and Kenyon, C. (2007). DAF-16/FOXO targets genes that regulate tumor growth in *Caenorhabditis elegans*. Nat. Genet. **39**:1403–1409.

Seale, M., and Bennett, T. (2017). BRC1 expression regulates bud activation potential but is not necessary or sufficient for bud growth inhibition in *Arabidopsis*. Development **144**:1661–1673.

Shabek, N., Ticchiarelli, F., Mao, H., Hinds, T.R., Leyser, O., and Zheng, N. (2018). Structural plasticity of D3-D14 ubiquitin ligase in strigolactone signalling. Nature **563**:652–656.

Smit, P., Raedts, J., Portyanko, V., Debelle, F., Gough, C., Bisseling, T., and Geurts, R. (2005). NSP1 of the GRAS protein family is essential for rhizobial Nod factor-induced transcription. Science **308**:1789–1791.

Song, X., Lu, Z., Hong, Y., Shao, G., Xiong, J., Meng, X., Jing, Y., Liu, G., Xiong, G., and Duan, J. (2017). IPA1 functions as a downstream transcription factor repressed by D53 in strigolactone signaling in rice. Cell Res. **27**:1128–1141.

Soundappan, I., Bennett, T., Morffy, N., Liang, Y., Stanga, J.P., Abbas, A., Leyser, O., and Nelson, D.C. (2015). SMAX1-LIKE/D53 family members enable distinct MAX2-dependent responses to strigolactones and karrikins in *Arabidopsis*. Plant Cell **27**:3143–3159.

Stanga, J.P., Smith, S.M., Briggs, W.R., and Nelson, D.C. (2013). SUPPRESSOR OF MORE AXILLARY GROWTH2 1 controls seed germination and seedling development in *Arabidopsis*. Plant Physiol. **163**:318–330.

Stanga, J.P., Morffy, N., and Nelson, D.C. (2016). Functional redundancy in the control of seedling growth by the karrikin signaling pathway. Planta **243**:1397–1406.

Sun, Y., Fan, X.Y., Cao, D.M., Tang, W., He, K., Zhu, J.Y., He, J.X., Bai, M.Y., Zhu, S., and Oh, E. (2010). Integration of brassinosteroid signal transduction with the transcription network for plant growth regulation in *Arabidopsis*. Dev. Cell **19**:765–777.

Tang, W., Yuan, M., Wang, R., Yang, Y., Wang, C., Oses-Prieto, J.A., Kim, T.W., Zhou, H.W., Deng, Z., Gampala, S.S., et al. (2011). PP2A activates brassinosteroid-responsive gene expression and plant growth by dephosphorylating BZR1. Nat. Cell Biol. **13**:124–131.

Tognetti, V.B., Van Aken, O., Morreel, K., Vandenbroucke, K., van de Cotte, B., De Clercq, I., Chiwocha, S., Fenske, R., Prinsen, E., Boerjan, W., et al. (2010). Perturbation of indole-3-butyric acid homeostasis by the UDP-glucosyltransferase UGT74E2 modulates *Arabidopsis* architecture and water stress tolerance. Plant Cell **22**:2660–2679.

Umehara, M., Hanada, A., Yoshida, S., Akiyama, K., Arite, T., Takeda-Kamiya, N., Magome, H., Kamiya, Y., Shirasu, K., Yoneyama, K., et al. (2008). Inhibition of shoot branching by new terpenoid plant hormones. Nature **455**:195–200.

Valverde, F., Mouradov, A., Soppe, W., Ravenscroft, D., Samach, A., and Coupland, G. (2004). Photoreceptor regulation of CONSTANS protein in photoperiodic flowering. Science **303**:1003–1006.

Vegh, A., Incze, N., Fabian, A., Huo, H., Bradford, K.J., Balazs, E., and Soos, V. (2017). Comprehensive analysis of DWARF14-LIKE2 (DLK2)

reveals its functional divergence from strigolactone-related paralogs. Front. Plant Sci. **8**:1641.

Wallner, E.S., Lopez-Salmeron, V., Belevich, I., Poschet, G., Jung, I., Grunwald, K., Sevilem, I., Jokitalo, E., Hell, R., Helariutta, Y., et al. (2017). Strigolactone- and karrikin-independent SMXL proteins are central regulators of phloem formation. Curr. Biol. **27**:1241–1247.

Wang, Y., Sun, S., Zhu, W., Jia, K., Yang, H., and Wang, X. (2013). Strigolactone/MAX2-induced degradation of brassinosteroid transcriptional effector BES1 regulates shoot branching. Dev. Cell **27**:681–688.

Wang, L., Wang, B., Jiang, L., Liu, X., Li, X., Lu, Z., Meng, X., Wang, Y., Smith, S.M., and Li, J. (2015). Strigolactone signaling in *Arabidopsis* regulates shoot development by targeting D53-like SMXL repressor proteins for ubiquitination and degradation. Plant Cell **27**:3128–3142.

Waters, M.T., Nelson, D.C., Scaffidi, A., Flematti, G.R., Sun, Y.K., Dixon, K.W., and Smith, S.M. (2012). Specialisation within the DWARF14 protein family confers distinct responses to karrikins and strigolactones in *Arabidopsis*. Development **139**:1285–1295.

Yang, M., and Wang, X. (2017). Multiple ways of BES1/BZR1 degradation to decode distinct developmental and environmental cues in plants. Mol. Plant **10**:915–917.

Yang, M., Li, C., Cai, Z., Hu, Y., Nolan, T., Yu, F., Yin, Y., Xie, Q., Tang, G., and Wang, X. (2017). SINAT E3 ligases control the light-mediated stability of the brassinosteroid-activated transcription factor BES1 in *Arabidopsis*. Dev. Cell **41**:47–58.e44.

Yao, R., Ming, Z., Yan, L., Li, S., Wang, F., Ma, S., Yu, C., Yang, M., Chen, L., and Chen, L. (2016). DWARF14 is a non-canonical hormone receptor for strigolactone. Nature **536**:469.

Yin, Y., Wang, Z.Y., Moragarcia, S., Li, J., Yoshida, S., Asami, T., and Chory, J. (2002). BES1 accumulates in the nucleus in response to brassinosteroids to regulate gene expression and promote stem elongation. Cell **109**:181–191.

Yin, Y., Vafeados, D., Tao, Y., Yoshida, S., Asami, T., and Chory, J. (2005). A new class of transcription factors mediates brassinosteroid-regulated gene expression in *Arabidopsis*. Cell **120**:249–259.

Zhou, F., Lin, Q., Zhu, L., Ren, Y., Zhou, K., Shabek, N., Wu, F., Mao, H., Dong, W., Gan, L., et al. (2013). D14-SCF(D3)-dependent degradation of D53 regulates strigolactone signalling. Nature **504**:406–410.

Plant Communications, Volume *1*

Supplemental Information

BES1 Functions as the Co-regulator of D53-like SMXLs to Inhibit *BRC1* Expression in Strigolactone-Regulated Shoot Branching in *Arabidopsis*

Jie Hu, Yuanyuan Ji, Xiaotong Hu, Shiyong Sun, and Xuelu Wang

Supplemental Figures and Tables

BES1 functions as co-regulator of D53-like SMXLs to inhibit *BRC1* expression in strigolactone-regulated shoot branching in *Arabidopsis*

Jie Hu[1], Yuanyuan Ji[1, 2], Xiaotong Hu[1], Shiyong Sun[1, *] and Xuelu Wang[1, *]

[1] National Key Laboratory of Crop Genetic Improvement and Center of Integrative Biology, College of Life Science and Technology, Huazhong Agricultural University, Wuhan, 430070 China

[2] Department of Genetics, School of Life Sciences, Fudan University, Shanghai, 200438 China

[*]Correspondence:

Xuelu Wang (Email: xlwang@mail.hzau.edu.cn, Tel: 86-27-87287166, FAX: 86-27-87287366) or Shiyong Sun (Email: sunshiyong@mail.hzau.edu.cn)

The supplemental file includes 10 Supplemental Figures and 7 Supplemental Tables.

SUPPLEMENTAL FIGURES

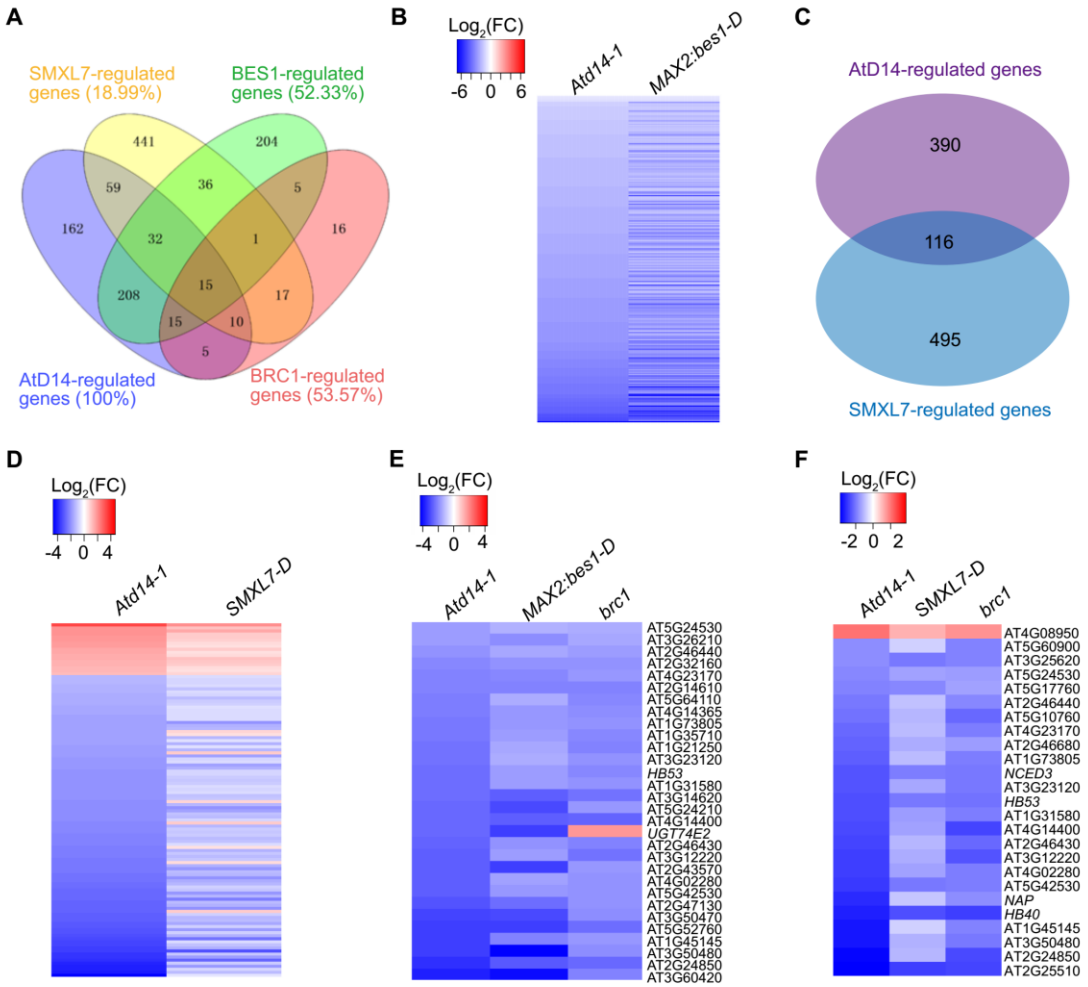

Supplemental Figure 1. Differential expression genes in the *Atd14-1*, *SMXL7-D*, *MAX2:bes1-D* and *brc1* plants, Related to Figure 1.

(A) Percentage in bracket indicated the portion of differential expression genes in *Atd14-1* plants, co-regulated by SMXL7, BES1 and BRC1, respectively, Related to Figure 1.

(B) Heatmap displayed the expression profiles of genes co-regulated by BES1 and AtD14. The colored bars indicated the original fold change values transformed by $\log_2$ regression.

(C) Venn diagram of the number of differentially expressed genes in buds of *Atd14-1*, and *SMXL7-D*, compared to Col-0.

(D) Heatmap showed the expression profiles of genes co-regulated by SMXL7 and AtD14. The colored bars indicated the original fold change values transformed by $\log_2$ regression.

(E) Heatmap showed the expression profiles of genes co-regulated by AtD14, BES1 and BRC1. The colored bars indicated the original fold change values transformed by log2 regression.

(F) Heatmap showed the expression profiles of genes co-regulated by AtD14, SMXL7 and BRC1. The colored bars indicated the original fold change values transformed by

$\log_2$ regression.
Differentially expressed genes in buds were obtained from cuffdiff analysis with q value < 0.05.

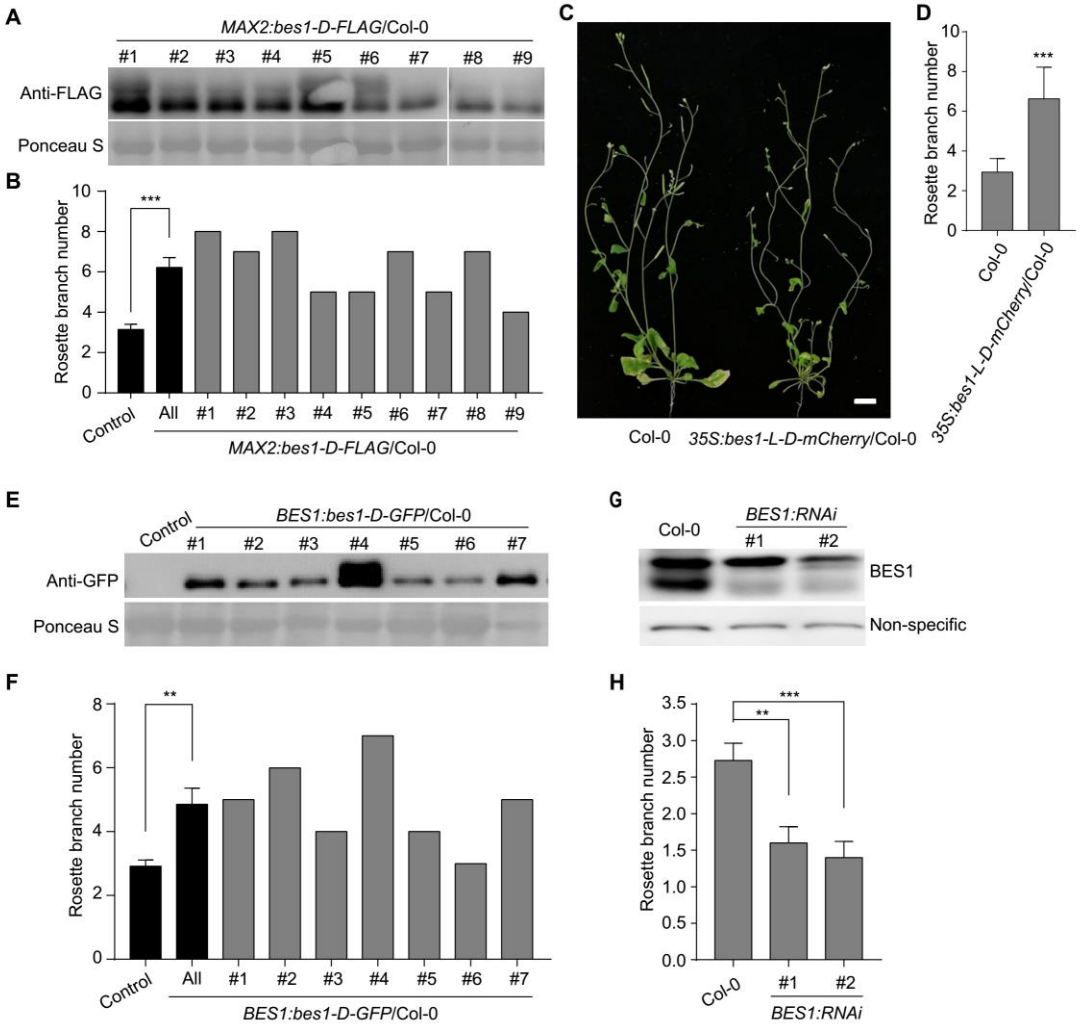

Supplemental Figure 2. BES1 plays an important role in branching in *Arabidopsis*, Related to Figure 1.

(A) The protein level of BES1-FLAG in leaves of *MAX2:bes1-D-FLAG*/Col-0 transgenic T1 lines was detected by anti-FLAG anti-body. Number #1-9 represented 9 independent T1 lines of *MAX2:bes1-D-FLAG*/Col-0.

(B) The corresponding rosette branch numbers of *MAX2:bes1-D-FLAG*/Col-0 lines in (A) were collected after their completed life cycle. The control was transgenic plants expressed empty vector (sample number of the Control was 12), "All" means all of the T1 lines, number #1-9 were indicated in (A).

(C&D) The enhanced branching phenotype(C) and rosette branch numbers (D) of *35S:bes1-L-D-mCherry*/Col-0 (sample number was 8) and Col-0 (sample number was 16). Branch numbers were collected after they completed their life cycle.

(E) The protein level of BES1-GFP in *BES1*:*bes1-D-GFP*/Col-0 transgenic T1 lines was detected by anti-GFP anti-body. Number #1-7 represented 7 independent T1 lines of *BES1*:*bes1-D-GFP*/Col-0.

(F) The corresponding rosette branch numbers of these *BES1:bes1-D-GFP*/Col-0 lines in (E) were collected after their complete life cycle. The control was transgenic

plants expressed empty vector (the sample number was 8), “All” means all of the T1 lines, number #1-7 were indicated in (E)

(G) The protein level of endogenous BES1 detected by anti-BES1 anti-body of 2 independent *BES1-RNAi* lines.

(H) The corresponding rosette branch numbers of wild type Col-0 and these 2 independent *BES1-RNAi* lines 6 weeks after transplant on soil (sample numbers were 11, 10 and 10, respectively).

Data were means ± SE. *P* values in (B, D, F, H) were determined by Student’s *t*-test; *** $P < 0.001$; ** $P < 0.01$.

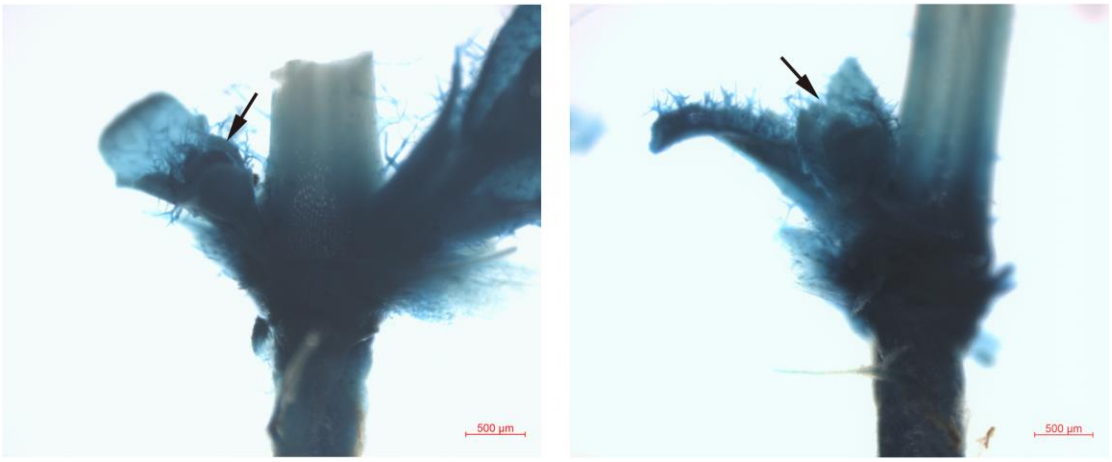

BES1p-L:GUS *BES1p-S:GUS*

Supplemental Figure 3. Both of the *BES1p-L:GUS* and *BES1p-S:GUS* are highly expressed in the axillary buds. Related to Figure 1.

Buds wrapped by young leaves are less than 0.5 mm and pointed by black arrows. Scar bar represent 500 μm.

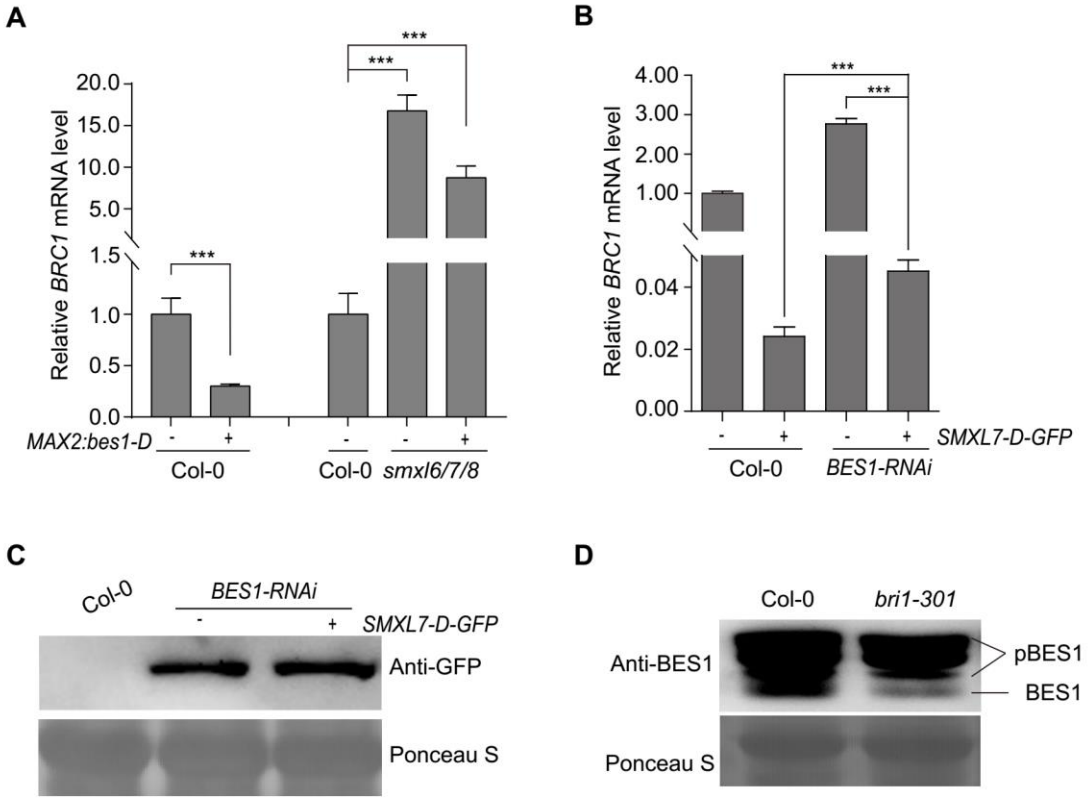

Supplemental Figure 4. Identification of the related protein and expression levels in transgenic plants, Related to Figure 1, 3 and 4.

(A) The transcription level of *BRC1* in *MAX2:bes1-D-FLAG* in Col-0 and *smxl6/7/8* background, and Col-0, *smxl6/7/8* lines, respectively.

(B) The transcription level of *BRC1* in *SMXL7-D-GFP*/Col-0 and *SMXL7-D-GFP /BES1-RNAi* background, Col-0 and *BES1-RNAi* lines.

(C) Immunoblotting revealed SMXL7-GFP levels was similar in *SMXL7-D-GFP*/Col-0 and *SMXL7-D-GFP/BES1-RNAi* transgenic lines using anti-GFP antibody. Ponceau S staining showed that equivalent amounts of loaded proteins were analyzed.

(D) Immunoblotting revealed the phosphorylated status of BES1 in Col-0 and *bri1-301* seedlings by endogenous anti-BES1 antibody. Ponceau S staining showed that equivalent amounts of loaded proteins were analyzed.

Data were means ± SD (n = 3). *P* values in (A and B) were determined by Student's *t*-test; *** $P < 0.001$.

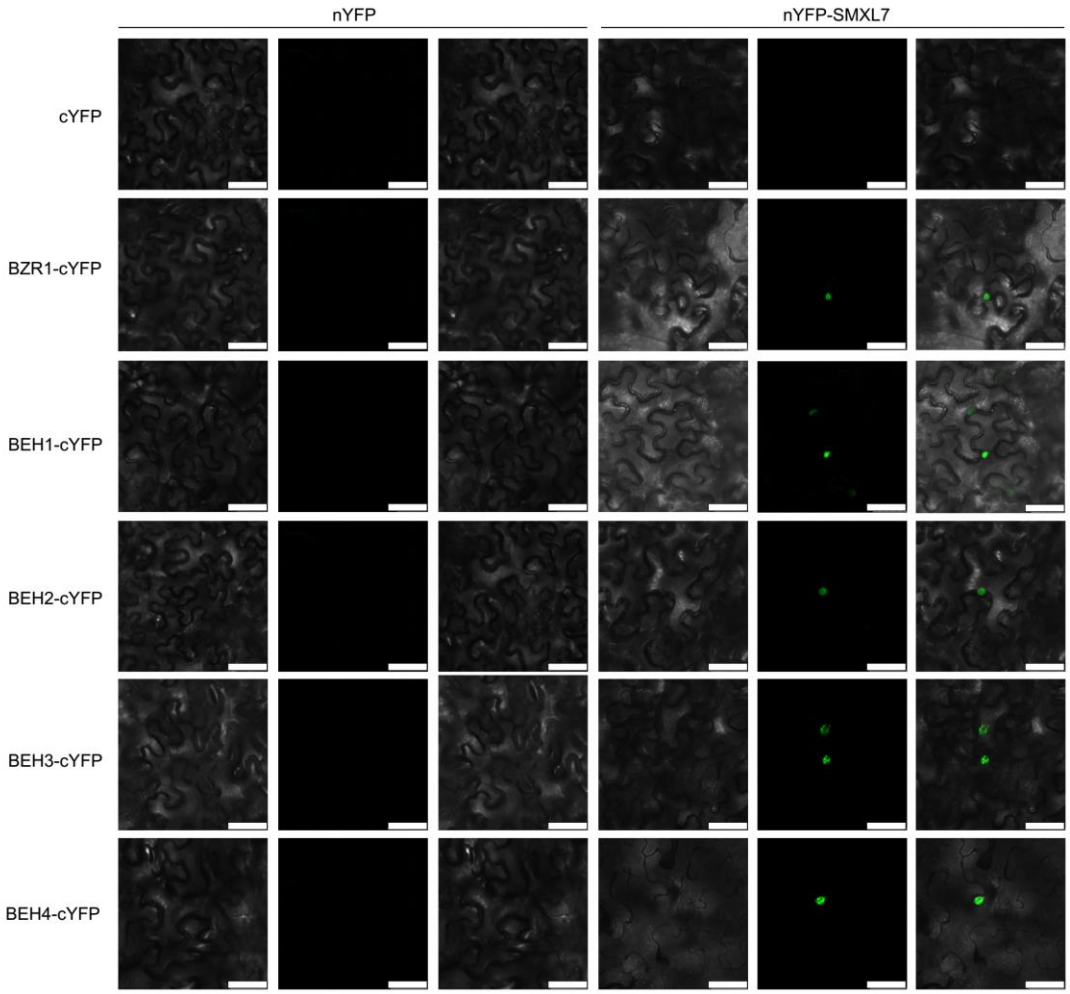

Supplemental Figure 5. SMXL7 interacts with the homologs of BES1, Related to Figure 2.

In bimolecular fluorescence complementation assays, SMXL7 interacted with the homologs of BES1. nYFP was fused to the N-terminus of SMXL7, and cYFP was linked to the C-terminus of BES1 homologs, including BZR1, BEH1, BEH2, BEH3, and BEH4, which were transiently co-expressed with nYFP-SMXL7 in *N. benthamiana* leaves. Scale bars represented 50 μm.

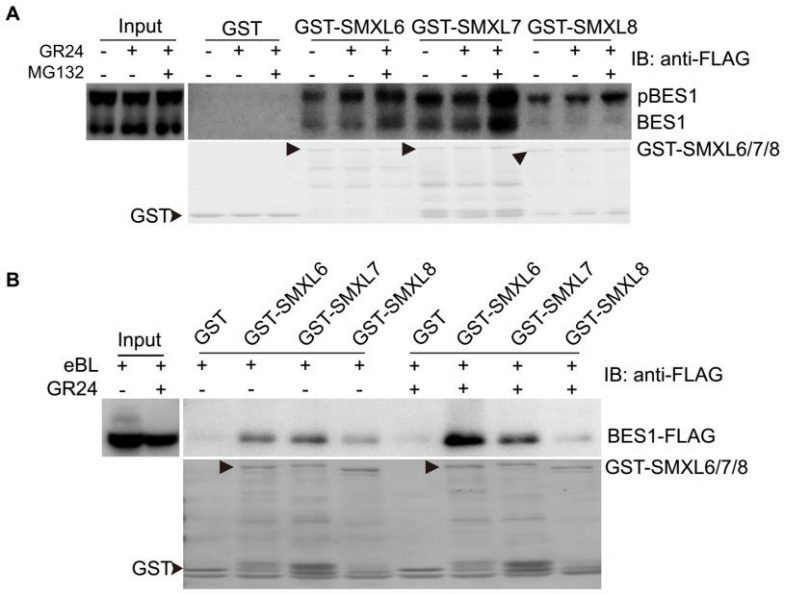

Supplemental Figure 6. BRs and SLs have no effect on the interaction between BES1 and SMXL7, Related to Figure 2.

(A) The interaction between BES1 and D53-like SMXLs was independent of GR24 treatment. 5 μM GR24 and 50 μM MG132 were added in the incubation of GST recombinant proteins and protein extraction of *35S:BES1-FLAG*/Col-0 plants.

(B) The interaction between BES1 and D53-like SMXLs was independent of eBL, and eBL plus GR24 treatment. The semi-*in vivo* pull-down assay used GST recombinant proteins, and protein extraction was from seedlings of *35S:BES1-FLAG*/Col-0 plants. 5 μM eBL and 5 μM eBL plus 5 μM GR24 treatment for 3 hrs were performed on the seedling of *35S:BES1-FLAG*/Col-0 plants before protein extraction and during the incubation of GST recombinant proteins and protein extraction of *35S:BES1-FLAG*/Col-0 plants.

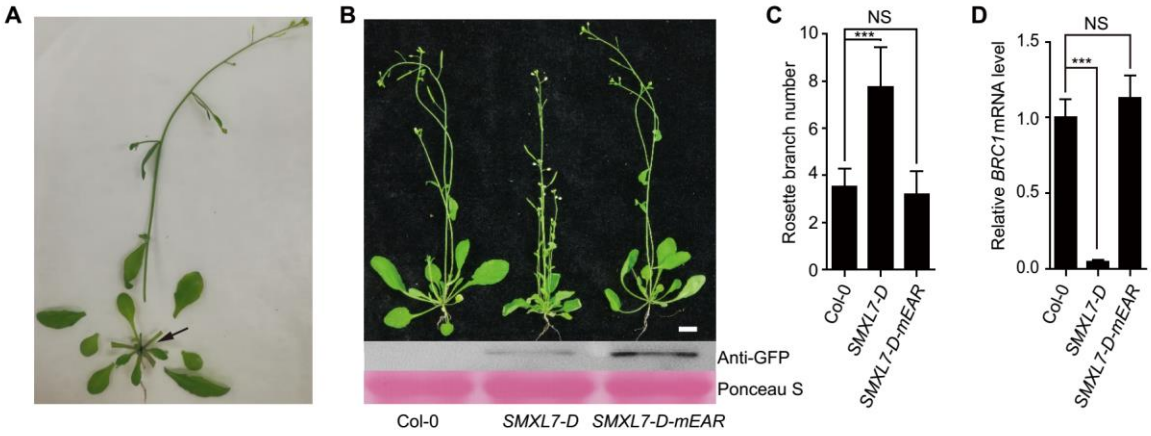

Supplemental Figure 7. The EAR motif of SMXLs is required to inhibit *BRC1* expression. Related to Figure 3.

(A) the shoot-root junction region of plants contained rosette buds without rosette leaves and large bud leaves used in ChIP assays (Black arrow pointed).
(**B&C**) Phenotypes and quantification of rosette branch number of Col-0, *SMXL7-D* and *SMXL7-D-mEAR* transgenic lines. bar = 1cm, (Col-0 (n = 15), *SMXL7-D* (n = 19) and *SMXL7-D-mEAR* (n = 26)).
(**D**) Relative expression levels of *BRC1* in Col-0, *SMXL7-D* and *SMXL7-D-mEAR* were determined by qRT-PCR.
Data were means ± SE in (C); data were means ± SD (n = 3) in (D). *P* values in (C and D) were determined by Student's *t*-test; *** $P < 0.001$; non-significant (NS), $P > 0.05$.

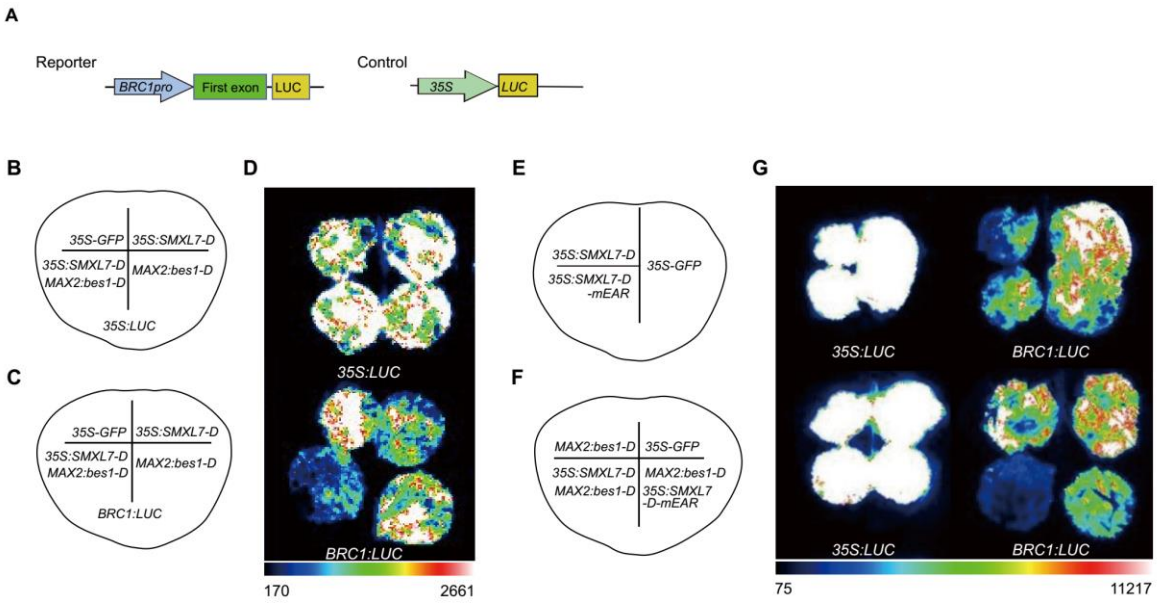

Supplemental Figure 8. The D53-like SMXLs and BES1 depend on each other to inhibit *BRC1* expression. Related to Figure 3.

(A) Schematic diagrams of the luciferase and control reporter in below transient expression assays.

(B&C&D) The LUC reporter system indicated *BRC1* was corporately inhibited by SMXL7 and BES1. Schematic representation in (B&C) showed the combinations of reporters and effectors in the corresponding position.

(E&F&G) The LUC reporter system indicated the EAR motif of SMXL7 was essential for inhibition of the luciferase activity of *BRC1:LUC* by the SMXL7–BES1 complex. Schematic representation in (E&F) showed the combinations of reporters, and effectors in the corresponding position.

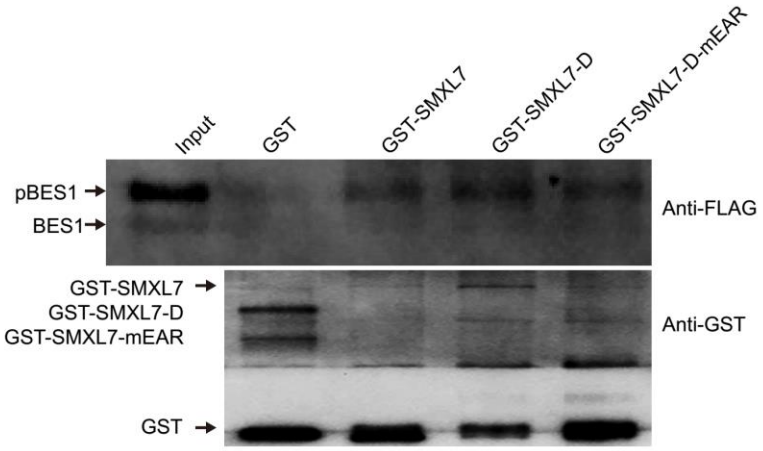

Supplemental Figure 9. BES1 interacts with SMXL7-D and SMXL7-D-mEAR, Related to Figure 3.

Semi-in vivo pull-down assay used glutathione-S-transferase (GST), GST-SMXL7, GST-SMXL7-D, and GST-SMXL7-D-mEAR recombinant proteins, and plant protein was extracted from *35S:BES1-FLAG* plants.

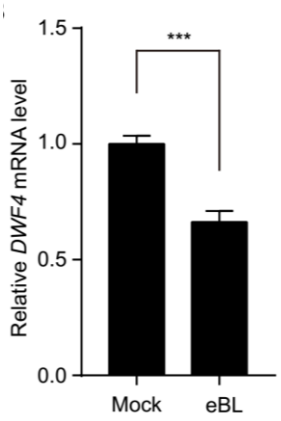

Supplemental Figure 10. Related to Figure 4. The transcription level of *DWF4* in buds of Col-0 under mock and 5 μM eBL treatments for 3 hrs. Data were means ± SD (n = 3). *P* values were determined by Student's *t*-test; *** $P < 0.001$.

Supplemental Table 1. Differential-expressed genes regulated by AtD14

Up-regulated genes in *Atd14-1* (VS Col-0)	Down-regulated genes in *Atd14-1*(VS Col-0)				
AT1G57750	AT4G33540	AT5G13220	AT2G29420	AT5G48430	AT3G46280
AT5G37940	AT3G15950	AT5G19230	AT4G36990	AT3G12220	AT2G34500
AT1G31690	AT3G23570	AT2G33380	AT4G32480	AT4G23230	AT5G38200
AT4G17860	AT5G55120	AT5G50200	AT2G41231	AT5G60270	AT3G59220
AT4G27570	AT1G60140	AT4G33050	AT2G43620	AT5G45380	AT2G15490
AT4G04840	AT4G27560	AT2G02010	AT1G15520	AT2G23680	AT5G13370
AT1G05540	AT1G70530	AT2G39710	AT1G58390	AT3G54420	AT3G48520
AT1G68600	AT1G68670	AT2G37040	AT5G42530	AT1G79410	AT5G52050
AT4G04955	AT2G34660	AT5G42830	AT3G47340	AT5G07010	AT4G15610
AT1G06350	ATMG00020	AT5G12170	AT5G63790	AT5G23660	AT1G43160
AT5G60490	AT1G69870	AT1G09970	AT1G35910	AT5G06860	AT1G01680
AT4G08950	AT4G22505	AT4G15120	AT5G26340	AT3G49780	AT1G05800
AT1G29660	AT3G06500	AT4G21380	AT3G05660	AT3G25730	AT1G07900
AT5G50790	AT4G21410	AT4G08870	AT1G21120	AT2G44790	AT1G13540
AT1G55330	AT2G13790	AT5G64110	AT5G08790	AT4G02280	AT1G18980
AT3G59010	AT2G36320	AT5G38940	AT3G48360	AT2G39980	AT1G28180
AT3G19680	AT5G55860	AT2G47000	AT3G24420	AT3G57260	AT1G33960
AT1G43790	AT1G58360	AT2G46440	AT2G26560	AT2G30140	AT1G62420
AT1G74670	AT1G17420	AT2G05380	AT4G26120	AT5G52760	AT1G70130
AT2G40460	AT5G19120	AT5G22270	AT5G17860	AT4G18170	AT1G73965
AT1G06360	AT5G13750	AT1G13990	AT5G49520	AT1G17170	AT2G14610
AT2G42990	AT5G36160	AT2G47800	AT4G19460	AT3G16530	AT2G31083
AT3G58120	AT5G51830	AT3G21670	AT4G14400	AT1G17180	AT2G42430
AT5G44680	AT2G41090	AT3G26210	AT2G38530	AT1G52890	AT2G44810
AT1G63710	AT1G01720	AT1G76680	AT1G21310	AT2G25510	AT2G47770
AT5G51890	AT3G05650	AT2G27310	AT5G16970	AT1G66480	AT3G02240
AT1G22160	AT1G54010	AT3G25780	AT5G35935	AT5G48657	AT3G11980
AT5G44020	AT2G23200	AT1G61820	AT2G36080	AT1G02920	AT3G46650
AT4G39800	AT1G49750	AT4G23170	AT1G70140	AT1G02930	AT3G49845
AT1G78020	AT4G15760	AT2G27500	AT2G43570	AT1G66760	AT4G04510
AT1G22530	AT1G72940	AT2G30400	AT1G01560	AT3G53480	AT4G04540
AT1G01600	AT3G23030	AT1G58340	AT5G36220	AT1G51800	AT4G13420
AT1G80280	AT3G21690	AT2G38860	AT4G23600	AT3G13790	AT4G22070
AT5G44130	AT2G22680	AT1G17830	AT5G49700	AT5G13330	AT4G27140
AT4G18970	AT5G57660	AT1G69730	AT3G22160	AT3G50470	AT5G07310
AT1G20850	AT2G29450	AT2G36800	AT3G16330	AT1G77450	AT5G10625
AT2G01420	AT4G34138	AT4G14365	AT2G28400	AT4G21120	AT5G12030
AT1G01120	AT1G76520	AT3G27025	AT1G12200	AT4G36740	AT5G16920
AT2G04070	AT2G46270	AT1G76590	AT3G13650	AT2G39030	AT5G52400
AT3G16680	AT5G53420	AT3G47780	AT5G15970	AT4G01870	AT5G64890
AT4G04000	AT1G32640	AT5G24290	AT2G18050	AT3G44860	AT5G66780
AT5G37970	AT5G05460	AT1G31580	AT2G37760	AT4G15530	AT4G39950
	AT4G17900	AT5G20230	AT3G04000	AT3G14440	AT5G52640
	AT3G51450	AT5G57480	AT1G59740	AT2G14560	AT2G43510
	AT2G31160	AT5G35735	AT3G55720	AT2G45570	AT2G41380
	AT5G67420	AT3G48990	AT3G48080	AT4G02520	AT1G64950
	AT1G80440	AT1G72120	AT1G05680	AT3G55970	AT4G31500
	AT2G43520	AT1G21250	AT5G66650	AT2G39200	AT1G64900
	AT1G25550	AT2G44290	AT5G47560	AT3G17609	AT5G22300
	AT3G13110	AT1G62940	AT4G25410	AT4G34710	AT4G22530
	AT4G37180	AT4G35110	AT4G08770	AT1G02850	AT1G02400
	AT3G53260	AT2G18660	AT1G73480	AT4G02380	AT1G69490
	AT1G08800	AT3G25610	AT1G75490	AT3G12580	AT3G19030
	AT4G34000	AT1G35710	AT1G16850	AT3G60420	AT3G50480
	AT3G13910	AT2G46680	AT5G05600	AT2G29440	AT3G50770
	AT5G11260	AT2G41510	AT5G07440	AT2G24850	AT3G50970
	AT1G17745	AT5G03700	AT5G14180	AT2G15480	AT5G15960
	AT1G17380	AT5G10760	AT5G04340	AT3G18550	AT1G16260
	AT4G36040	AT4G37370	AT1G66920	AT1G74010	AT3G44720
	AT5G61010	AT3G57240	AT2G39210	AT1G32960	AT1G69850
	AT2G26530	AT4G13180	AT5G25440	AT3G63380	AT3G28930
	AT1G60730	AT3G46660	AT5G46050	AT5G55050	AT5G66700
	AT1G59700	AT5G60950	AT1G49500	AT1G55920	AT5G60900
	AT4G21400	AT2G20670	AT2G27690	AT3G26830	AT1G72900
	AT5G19440	AT5G49480	AT1G34420	AT5G49690	AT1G56650
	AT3G49120	AT3G21230	AT5G24210	AT4G08555	AT4G34135
	AT3G51430	AT5G14780	AT5G61820	AT1G76930	AT2G46430
	AT4G28490	AT2G36950	AT1G14870	AT1G80820	AT1G45145
	AT4G17500	AT2G27830	AT5G11410	AT3G15500	AT5G25250
	AT1G49050	AT4G18360	AT3G14620	AT1G69930	AT2G37770
	AT5G54170	AT2G32160	AT1G10340	AT4G22710	AT2G29460
	AT1G73500	AT3G03990	AT1G52200	AT3G54150	AT3G23250
	AT5G54510	AT2G15760	AT3G23120	AT3G44300	AT3G49620
	AT2G37180	AT5G39050	AT2G47130	AT1G77760	
	AT1G50420	AT4G38540	AT5G39610	AT1G02360	
	AT4G19700	AT1G73805	AT2G18690	AT4G36850	

Supplemental Table 2. Differential-expressed genes regulated by BES1

Up-regulated genes in *MAX2:bes1-D* (VS Col-0)	Down-regulated genes in *MAX2:bes1-D* (VS Col-0)						
AT1G19350	AT1G20440	AT5G52640	AT1G08050	AT2G36950	AT2G47000	AT4G25810	AT3G60120
AT2G41640	AT4G16990	AT1G31580	AT4G18360	AT5G10380	AT4G25410	AT1G72920	AT4G06746
AT4G25100	AT2G44490	AT4G37410	AT1G18590	AT5G26920	AT4G30270	AT4G34135	AT4G08040
AT5G42800	AT2G26190	AT3G16670	AT3G16720	AT5G01100	AT1G76070	AT2G41100	AT4G11480
AT1G67750	AT3G49120	AT5G53290	AT1G56660	AT1G63720	AT2G41231	AT3G15356	AT4G12490
AT4G00870	AT2G39570	AT5G56980	AT3G25760	AT5G05440	AT2G36970	AT3G52450	AT4G12500
AT4G34760	AT2G29450	AT3G13110	AT1G34420	AT5G49520	AT2G39210	AT1G55920	AT4G13420
AT2G16586	AT5G04720	AT5G46330	AT2G30870	AT5G11410	AT5G65300	AT5G35735	AT4G16260
AT3G07010	AT3G03780	AT4G02940	AT3G10985	AT4G08870	AT1G61560	AT2G45570	AT4G21830
AT4G02290	AT1G69870	AT3G23120	AT2G46430	AT2G43590	AT1G25400	AT1G14870	AT4G22070
AT4G00820	AT1G01720	AT1G26930	AT1G21130	AT4G18010	AT2G36380	AT3G13790	AT4G27140
AT4G20320	AT5G27760	AT3G57520	AT5G20480	AT5G49700	AT1G31540	AT5G13330	AT4G31950
AT2G03821	AT3G50950	AT1G17860	AT3G30775	AT4G20830	AT5G05690	AT2G29440	AT4G37990
AT4G22080	AT5G03380	AT1G72450	AT1G76590	AT2G39400	AT5G23510	AT5G24210	AT5G05300
AT5G58360	AT5G22920	AT2G46440	AT1G45145	AT1G66760	AT4G39070	AT1G65390	AT5G07100
	AT4G24160	AT1G72680	AT1G72520	AT1G79410	AT4G35770	AT2G44790	AT5G15130
	AT5G24530	AT5G42530	AT5G47560	AT5G14780	AT5G54710	AT3G60420	AT5G17350
	AT1G32700	AT3G54640	AT1G73480	AT4G24040	AT1G68620	AT3G15500	AT5G17390
	AT3G16420	AT4G17250	AT3G22370	AT5G49480	AT2G32150	AT3G50480	AT5G22540
	AT2G43520	AT2G36080	AT2G18193	AT1G73500	AT3G25780	AT2G39200	AT5G46295
	AT3G57450	AT4G29780	AT4G34230	AT2G36800	AT5G26340	AT1G66480	AT5G64890
	AT1G49050	AT5G65380	AT5G13200	AT1G10370	AT1G72930	AT1G27730	AT1G05010
	AT3G15210	AT2G31750	AT4G01010	AT1G77450	AT4G35110	AT5G49690	AT1G61890
	AT5G67300	AT3G05660	AT4G39950	AT5G13220	AT2G43510	AT5G64120	AT5G18130
	AT4G28490	AT1G21000	AT2G32160	AT3G61280	AT1G76650	AT3G55970	AT3G10340
	AT5G13750	AT3G23030	AT5G41740	AT2G47130	AT5G39610	AT3G50970	AT1G11580
	AT3G13520	AT3G62150	AT5G14120	AT5G46050	AT3G63380	AT3G59220	AT4G19880
	AT4G15490	AT2G46600	AT1G60730	AT3G26210	AT4G17500	AT2G34500	AT4G27300
	AT5G64110	AT4G02280	AT2G40000	AT3G23570	AT1G15125	AT4G21120	AT1G72120
	AT2G23810	AT1G35710	AT1G75750	AT4G23600	AT4G01750	AT2G19800	AT1G51760
	AT1G54020	AT5G05730	AT1G19380	AT1G72910	AT5G16970	AT5G20230	AT1G21010
	AT4G36648	AT3G51600	AT4G23170	AT1G09970	AT3G21230	AT5G05600	AT2G48020
	AT2G43910	AT2G24100	AT1G06620	AT2G35930	AT3G17609	AT5G04340	AT3G18830
	AT1G20510	AT5G66700	AT3G28930	AT3G26220	AT3G04210	AT1G76930	AT3G20660
	AT5G06870	AT1G70700	AT5G25440	AT2G37040	AT1G02930	AT4G15530	AT5G39020
	AT1G21250	AT3G55980	AT5G48540	AT5G36220	AT1G76680	AT1G80820	AT4G22530
	AT1G54010	AT1G57990	AT3G21240	AT3G46110	AT1G70140	AT2G37770	AT2G38860
	AT5G38940	AT4G39940	AT3G22060	AT5G45340	AT3G47340	AT2G26560	AT5G57785
	AT3G45640	AT1G75040	AT1G74100	AT2G22470	AT1G62300	AT4G02380	AT1G61820
	AT1G70530	AT4G15760	AT2G43620	AT1G72940	AT1G19180	AT3G49620	AT4G36670
	AT3G50660	AT5G52310	AT1G68840	AT3G16330	AT5G22270	AT4G02520	AT1G37130
	AT3G51450	AT4G14365	AT5G39050	AT2G44080	AT5G08790	AT5G52050	AT3G19030
	AT3G05200	AT3G56400	AT2G16060	AT1G75490	AT1G28370	AT3G01290	AT4G13395
	AT5G42650	AT5G61600	AT3G46660	AT5G12170	AT5G52760	AT2G15480	AT3G22160
	AT1G28130	AT5G44260	AT3G54140	AT2G18660	AT2G02010	AT3G26830	AT4G36850
	AT5G05140	AT4G31500	AT1G02400	AT5G27420	AT4G01870	AT2G29460	AT3G52400
	AT1G03220	AT3G47420	AT5G59540	AT2G37760	AT4G18170	AT3G23250	AT1G15520
	AT5G05460	AT5G63160	AT4G22690	AT3G12580	AT2G30140	AT1G02920	AT4G13180
	AT1G13990	AT1G17380	AT5G61820	AT3G13650	AT5G15960	AT3G16530	AT1G72900
	AT5G06320	AT4G23270	AT1G76520	AT3G18550	AT2G43570	AT1G43160	AT5G07010
	AT1G11330	AT5G17000	AT1G71880	AT5G46350	AT5G13370	AT1G05800	AT1G17170
	AT5G01210	AT3G12220	AT3G50760	AT2G39980	AT3G48650	AT1G07160	AT1G27020
	AT1G68440	AT1G12110	AT4G36500	AT1G76600	AT1G02850	AT1G07900	AT5G55050
	AT1G64950	AT1G73805	AT1G08930	AT3G47780	AT2G27690	AT1G08090	AT1G05680
	AT4G27830	AT4G17900	AT3G25610	AT5G19240	AT3G50470	AT1G13480	AT1G18570
	AT3G59140	AT4G21850	AT1G23850	AT2G29420	AT3G22910	AT1G13520	AT2G25735
	AT2G30600	AT2G46650	AT5G60950	AT1G78000	AT3G54420	AT1G18980	AT2G39530
	AT3G13080	AT4G17490	AT2G24600	AT5G41750	AT3G24420	AT1G20310	AT2G41800
	AT1G13260	AT3G53260	AT4G06744	AT2G15042	AT4G38540	AT1G26390	AT3G04420
	AT1G22890	AT5G56870	AT2G22770	AT2G27500	AT5G60270	AT1G28180	AT3G19615
	AT1G17420	AT3G28220	AT2G30400	AT5G44380	AT4G33050	AT1G30720	AT3G43250
	AT4G17230	AT5G51830	AT4G32870	AT3G25770	AT2G23680	AT1G32350	AT3G48850
	AT5G17380	AT2G27830	AT1G52890	AT5G07440	AT5G17860	AT1G36622	AT3G52748
	AT1G01470	AT4G36990	AT1G18390	AT2G26530	AT5G45380	AT1G51890	AT1G21400
	AT5G19440	AT5G49730	AT5G63790	AT3G13950	AT5G40780	AT1G57650	AT3G21690
	AT4G31800	AT5G53550	AT3G48990	AT3G01970	AT5G50200	AT1G79680	AT4G37370
	AT4G21380	AT1G51680	AT3G16660	AT4G14400	AT1G24147	AT2G02930	AT5G47220
	AT2G40140	AT4G37610	AT1G59740	AT5G52750	AT1G66160	AT2G14610	AT5G19230
	AT5G54170	AT2G25450	AT2G43820	AT3G04720	AT2G27310	AT2G15390	AT2G36690
	AT5G54500	AT1G44350	AT2G30250	AT2G15760	AT1G77760	AT2G17740	
	AT3G49110	AT5G20250	AT3G04000	AT2G24850	AT5G06860	AT2G32660	
	AT4G30530	AT1G78850	AT4G19810	AT2G38470	AT3G14620	AT2G35980	

Supplemental Table 3. Differential-expressed genes co-regulated by AtD14-BES1

Up-regulated genes	Down-regulated genes			
N/A	AT3G23570	AT2G22770	AT4G23600	AT1G80820
	AT1G70530	AT3G25770	AT5G49700	AT3G15500
	AT1G69870	AT5G13220	AT3G22160	AT1G77760
	AT1G17420	AT5G19230	AT3G16330	AT4G36850
	AT5G13750	AT5G50200	AT3G13650	AT2G37770
	AT5G51830	AT4G33050	AT2G37760	AT2G29460
	AT1G01720	AT2G02010	AT3G04000	AT3G23250
	AT1G54010	AT2G37040	AT1G59740	AT3G49620
	AT4G15760	AT5G12170	AT1G05680	AT3G50970
	AT1G72940	AT1G09970	AT5G47560	AT5G15960
	AT3G23030	AT4G21380	AT4G25410	AT2G34500
	AT3G21690	AT4G08870	AT1G73480	AT3G59220
	AT2G29450	AT5G64110	AT1G75490	AT5G13370
	AT1G76520	AT5G38940	AT5G05600	AT5G52050
	AT5G05460	AT2G47000	AT5G07440	AT1G43160
	AT4G17900	AT2G46440	AT5G04340	AT1G05800
	AT3G51450	AT5G22270	AT2G39210	AT1G07900
	AT2G43520	AT1G13990	AT5G25440	AT1G18980
	AT3G13110	AT3G26210	AT5G46050	AT1G28180
	AT3G53260	AT1G76680	AT2G27690	AT2G14610
	AT1G17380	AT2G27310	AT1G34420	AT4G13420
	AT2G26530	AT3G25780	AT5G24210	AT4G22070
	AT1G60730	AT1G61820	AT5G61820	AT4G27140
	AT5G19440	AT4G23170	AT1G14870	AT5G64890
	AT3G49120	AT2G27500	AT5G11410	AT4G20830
	AT4G28490	AT2G30400	AT3G14620	AT5G40780
	AT4G17500	AT2G38860	AT3G23120	AT3G21240
	AT1G49050	AT2G36800	AT2G47130	AT5G59540
	AT5G54170	AT4G14365	AT5G39610	AT1G18570
	AT1G73500	AT1G76590	AT4G34135	AT5G41750
	AT3G28930	AT3G47780	AT2G46430	AT4G24040
	AT1G64950	AT1G31580	AT1G45145	AT5G52750
	AT4G31500	AT5G20230	AT3G19030	AT5G17860
	AT4G39950	AT5G35735	AT3G50480	AT5G49520
	AT1G74100	AT3G48990	AT2G43510	AT4G14400
	AT1G10370	AT1G72120	AT3G12220	AT5G16970
	AT4G34230	AT1G21250	AT5G60270	AT2G36080
	AT2G44080	AT4G35110	AT5G45380	AT1G70140
	AT5G24530	AT2G18660	AT2G23680	AT2G43570
	AT4G27830	AT3G25610	AT3G54420	AT5G36220
	AT1G21000	AT1G35710	AT1G79410	AT2G15480
	AT1G27020	AT4G37370	AT5G07010	AT3G18550
	AT1G72680	AT4G13180	AT5G06860	AT3G63380
	AT1G51760	AT3G46660	AT2G44790	AT5G55050
	AT3G20660	AT5G60950	AT4G02280	AT1G55920
	AT5G17000	AT5G49480	AT2G39980	AT3G26830
	AT3G50950	AT3G21230	AT2G30140	AT5G49690
	AT1G44350	AT5G14780	AT5G52760	AT1G76930
	AT1G06620	AT2G36950	AT4G18170	AT1G19180
	AT2G31750	AT2G27830	AT1G17170	AT5G53290
	AT5G47220	AT4G18360	AT3G16530	AT3G46110
	AT4G37410	AT2G32160	AT1G52890	AT1G18390
	AT1G32700	AT2G15760	AT1G66480	AT1G72930
	AT3G25760	AT5G39050	AT1G02920	AT5G26340
	AT4G15490	AT4G38540	AT1G02930	AT3G05660
	AT5G27420	AT1G73805	AT1G66760	AT5G08790
	AT1G26930	AT5G66700	AT3G13790	AT3G24420
	AT2G32150	AT1G72900	AT5G13330	AT2G26560
	AT5G01210	AT4G22530	AT3G50470	AT4G02380
	AT3G10985	AT1G02400	AT1G77450	AT3G12580
	AT3G22060	AT5G52640	AT4G21120	AT3G60420
	AT4G06744	AT2G29420	AT4G01870	AT2G29440
	AT3G56400	AT4G36990	AT4G15530	AT2G24850
	AT3G15356	AT2G41231	AT2G45570	AT5G19240
	AT1G62300	AT2G43620	AT4G02520	AT2G24100
	AT3G01290	AT1G15520	AT3G55970	AT3G47340
	AT5G52310	AT5G42530	AT2G39200	AT5G63790
	AT3G17609	AT1G02850		

Supplemental Table 4. Differential-expressed genes regulated by SMXL7

Up-regulated genes in *SMXL7-D* (VS Col-0)				Down-regulated genes in *SMXL7-D* (VS Col-0)				
AT5G03545	AT4G25430	AT2G41990	AT5G50150	AT1G07420	AT2G19450	AT4G26530	AT5G10760	AT1G61070
AT4G25010	AT5G65040	AT1G10990	AT5G18670	AT4G35090	AT3G59350	AT5G19120	AT5G15970	AT3G44042
AT1G06830	AT1G28010	AT3G24340	AT1G70090	AT4G22990	AT3G10410	AT3G63160	AT5G40730	AT1G75790
AT2G30766	AT1G69760	AT5G12050	AT1G05010	AT3G46970	AT3G05640	AT5G24770	AT4G11310	AT5G53190
AT5G51190	AT4G08950	AT4G31910	AT4G18970	AT1G77760	AT1G26450	AT2G35950	AT1G73805	AT4G10850
AT1G57750	AT1G08930	AT1G66940	AT3G02550	AT2G47850	AT3G05650	AT3G43670	AT3G26280	AT3G42960
AT3G16150	AT1G22160	AT2G38470	AT4G12870	AT4G14270	AT5G59670	AT5G52390	AT5G51210	AT3G18550
AT3G62150	AT5G64850	AT2G44500	AT4G27450	AT1G56220	AT2G15970	AT1G76790	AT4G14400	AT3G60280
AT1G68840	AT5G62280	AT3G16670	AT1G70940	AT2G04360	AT3G51000	AT3G62740	AT1G35720	AT1G22015
AT4G11460	AT5G07000	AT5G05250	AT1G67900	AT2G42610	AT5G24150	AT2G32530	AT5G17760	AT2G31083
AT2G40330	AT1G68600	AT1G06080	AT5G43700	AT4G26670	AT3G14360	AT3G41768	AT1G35910	AT2G31085
AT1G26680	AT1G05490	AT5G63850	AT5G23530	AT2G29310	AT4G27520	AT2G34655	AT1G65800	AT2G21100
AT4G08300	AT3G45160	AT1G20390	AT1G76090	AT5G26570	AT3G14595	AT1G02850	AT5G60100	AT1G66380
AT5G38710	AT5G52882	AT5G64770	AT4G00872	AT1G22770	AT2G39310	AT2G33380	AT1G52890	AT1G13930
AT5G60780	AT3G20395	AT4G15430	AT3G49580	AT1G13270	AT5G15780	AT1G08890	AT2G20670	AT2G47800
AT5G15830	AT1G13245	AT4G17670	AT1G61563	AT5G66040	AT1G30040	AT5G52310	AT2G40750	AT5G61380
AT2G25735	AT3G02140	AT2G45685	AT5G44680	AT5G62720	AT3G50950	AT3G29575	AT1G66760	AT5G44572
AT3G46490	AT2G29970	AT2G46450	AT1G55330	AT2G36350	AT1G16110	AT4G34710	AT2G41510	AT2G40100
AT4G38340	AT3G02380	AT5G48490	AT1G23090	AT5G38980	AT5G55450	AT1G56300	AT3G12220	AT5G03350
AT4G24570	AT5G24860	AT2G45180	AT2G24490	AT4G27130	AT3G05880	AT1G06460	AT5G42530	AT1G17600
AT3G52450	AT5G08170	AT1G70560	AT5G52860	AT1G20840	AT1G66970	AT3G05660	AT5G23240	AT1G70430
AT4G27280	AT1G15210	AT4G24240	AT5G47910	AT4G09020	AT1G29395	AT5G57340	AT3G30720	AT3G20810
AT1G76650	AT2G31110	AT4G32890	AT3G54500	AT3G46640	AT1G07440	AT3G61198	AT2G42540	AT5G60900
AT4G38830	AT1G25560	AT5G42650	AT2G23170	AT2G37200	AT5G57110	AT3G16450	AT2G36270	AT4G17090
AT3G22540	AT4G36880	AT5G63180	AT4G17460	AT5G42825	AT4G34000	AT4G08870	AT5G18600	AT1G07430
AT1G12110	AT2G02010	AT4G27300	AT5G64570	AT2G25730	AT3G45140	AT2G39800	AT3G23120	AT5G52160
AT3G05727	AT4G18010	AT1G73540	AT4G22490	AT2G21620	AT4G16690	AT5G62360	AT1G23840	AT1G62940
AT5G05440	AT1G28660	AT2G43100	AT5G50200	AT1G64900	AT2G23200	AT3G09790	AT4G04330	AT4G14080
AT4G21870	AT4G22517	AT3G23050	AT2G38940	AT5G24060	AT4G11600	AT1G62290	AT2G46430	AT5G07230
AT4G13575	AT3G16660	AT5G10770	AT4G21850	AT3G53980	AT5G06370	AT1G21310	AT1G73325	AT5G49730
AT1G65390	AT3G19680	AT5G01810	AT2G41100	AT2G15890	AT5G14780	AT2G44290	AT2G40080	AT4G27560
AT5G04190	AT1G44800	AT1G52190	AT3G24420	AT3G62410	AT3G05800	AT5G24470	AT3G62730	AT2G40300
AT1G73330	AT3G26760	AT4G35900	AT2G27402	AT1G80480	AT2G38530	AT5G56840	AT3G28270	AT3G01500
AT1G03170	AT5G64660	AT1G67860	AT3G01490	AT3G26740	AT5G19260	AT4G37180	AT2G18050	AT2G40400
AT2G38310	AT4G39800	AT3G55120	AT4G12910	AT4G12290	AT4G34950	AT1G04620	AT1G16850	AT4G37410
AT4G22520	AT2G40610	AT2G38120	AT1G76240	AT5G27660	AT5G38430	AT5G59220	AT4G02280	AT1G22890
AT1G58370	AT5G19190	AT1G21830	AT1G01120	AT5G06870	AT2G22450	AT1G03400	AT3G02480	AT1G69730
AT5G44380	AT5G61600	AT3G56360	AT3G50060	AT4G19700	AT1G72180	AT2G39710	AT3G22235	AT1G11175
AT2G41640	AT1G16390	AT5G48570	AT5G07580	AT3G56090	AT2G40970	AT2G37760	AT4G32340	AT1G49750
AT4G04955	AT2G44080	AT1G76680	AT3G05900	AT4G39090	AT5G23380	AT2G42530	AT5G66700	AT2G40130
AT1G24530	AT3G05140	AT2G27990	AT3G10040	AT1G04990	AT3G47860	AT2G46440	AT5G13370	AT3G42806
AT3G44260	AT3G27690	AT5G46790	AT2G41050	AT1G07200	AT1G21680	AT5G51720	AT3G25620	AT5G24780
AT1G01060	AT2G30520	AT5G40450	AT3G46620	AT5G20630	AT2G47890	AT3G50480	AT1G52770	AT3G09390
AT5G45340	AT3G26200	AT3G46600	AT1G02190	AT2G43535	AT3G27870	AT2G36885	AT5G19110	AT2G22980
AT1G43800	AT1G28670	AT5G15850	AT3G17330	AT3G05980	AT1G58340	AT2G46680	AT1G19960	AT2G21130
AT4G29780	AT4G17870	AT3G58120	AT4G25750	AT3G04550	AT1G48330	AT4G23170	AT2G24850	AT4G30650
AT4G18290	AT1G73600	AT2G28305	AT3G55980	AT2G28900	AT4G15210	AT4G21380	AT2G39855	AT5G44050
AT5G57560	AT4G14130	AT4G27310	AT4G22513	AT4G27830	AT1G78850	AT1G74890	AT5G59310	AT1G12160
AT4G30140	AT2G23290	AT1G09420	AT3G12320	AT2G14878	AT5G48250	AT5G42750	AT4G33980	AT1G17830
AT5G16570	AT2G34430	AT5G15120	AT1G44100	AT1G26665	AT5G13320	AT4G25480	AT3G47340	AT1G76590
AT5G46240	AT5G07690	AT1G32900	AT5G07460	AT5G67480	AT2G23910	AT5G03840	AT1G07050	AT4G11350
AT2G28780	AT2G06200	AT3G06070	AT1G14430	AT1G05500	AT5G01600	AT2G28160	AT4G25100	AT5G61820
AT2G46830	AT5G59050	AT2G43290	AT4G28680	AT2G41090	AT3G60670	AT1G73480	AT1G68050	AT1G12010
AT2G37460	AT1G57990	AT5G22500	AT4G12980	AT4G04630	AT4G31620	AT1G17665	AT5G66400	AT4G16146
AT1G13260	AT3G05730	AT5G15950	AT1G73590	AT3G51430	AT3G57010	AT3G60700	AT1G11210	AT4G32480
AT2G36120	AT1G78020	AT3G05600	AT5G22580	AT5G54510	AT1G49500	AT1G52100	AT2G25510	AT2G21660
AT5G59780	AT5G61590	AT1G29660	AT4G13495	AT5G36160	AT2G05380	AT1G67260	AT2G33830	AT4G16590
AT1G34060	AT2G42380	AT5G45720	AT1G70260	AT5G21430	AT1G01470	AT1G31580	AT4G36850	AT1G09500
AT5G34795	AT5G65080	AT5G03610	AT4G17490	AT5G54960	AT3G07650	AT3G49120	AT2G18550	AT4G23600
AT5G43580	AT5G37770	AT1G73500	AT4G17860	AT3G53460	AT4G00165	AT1G79520	AT3G14440	AT1G28375
AT4G14140	AT3G20470	AT1G37130	AT3G15540	AT1G44350	AT4G11900	AT5G24530	AT5G42900	AT1G58225
AT1G07135	AT4G17500	AT1G22530	AT4G33790	AT1G50420	AT1G75750	AT2G29340	AT2G39510	AT1G66850
AT5G34800	AT5G61660	AT5G11950	AT4G11280	AT1G45145	AT1G69490	AT5G57630	AT3G27250	AT3G07450
AT3G28345	AT2G30010	AT1G04240	AT5G06980	AT5G08260	AT1G79440	AT5G28910	AT3G22231	AT3G17520
AT1G03870	AT1G06350	AT2G23810	AT5G44630	AT1G71050	AT4G15440	AT4G15490	AT4G36740	AT4G29980
AT4G20070	AT5G37600	AT2G40000	AT5G07800	AT3G43270	AT4G37540	AT2G32540	AT4G21930	AT4G32105
AT5G39890	AT3G23430	AT1G17920	AT2G32560	AT2G01150	AT4G16190	AT3G19200	AT1G44970	AT5G05220
AT4G22780	AT2G37040			AT2G31200	AT3G24520	AT4G16270	AT1G04645	AT5G24820
								AT5G25950

Supplemental Table 5. Differential-expressed genes co-regulated by AtD14-SMXL7

Up-regulated genes in both of *SMXL7-D* and *AtD14-1*	Down-regulated genes in both of *SMXL7-D* and *AtD14-1*		Down-regulated genes in *AtD14-1* But up-regulated in *SMXL7-D*
AT1G57750	AT1G77760	AT3G50480	AT5G50200
AT4G04955	AT1G64900	AT2G46680	AT3G24420
AT4G17860	AT4G19700	AT4G23170	AT2G02010
AT4G08950	AT4G27830	AT4G21380	AT2G44080
AT1G22160	AT2G41090	AT1G73480	AT4G17500
AT1G68600	AT3G51430	AT1G31580	AT1G76680
AT3G19680	AT5G54510	AT3G49120	AT1G73500
AT4G39800	AT5G36160	AT5G24530	AT2G37040
AT1G78020	AT1G44350	AT2G29340	
AT1G06350	AT1G50420	AT4G15490	
AT1G01120	AT1G45145	AT1G76590	
AT3G58120	AT4G27560	AT5G61820	
AT1G29660	AT4G37410	AT4G32480	
AT1G22530	AT1G69730	AT4G23600	
AT5G44680	AT1G49750	AT5G60900	
AT1G55330	AT2G47800	AT5G10760	
AT4G18970	AT3G05650	AT5G15970	
	AT3G50950	AT1G73805	
	AT4G34000	AT4G14400	
	AT4G16690	AT5G17760	
	AT2G23200	AT1G35910	
	AT5G14780	AT1G52890	
	AT2G38530	AT2G20670	
	AT1G58340	AT2G40750	
	AT1G49500	AT1G66760	
	AT2G05380	AT2G41510	
	AT1G69490	AT3G12220	
	AT4G37540	AT5G42530	
	AT1G17830	AT2G42540	
	AT5G19120	AT2G36270	
	AT1G02850	AT3G23120	
	AT2G33380	AT2G46430	
	AT5G52310	AT2G18050	
	AT4G34710	AT1G16850	
	AT3G05660	AT4G02280	
	AT4G08870	AT5G66700	
	AT1G21310	AT5G13370	
	AT2G44290	AT3G25620	
	AT4G37180	AT3G47340	
	AT5G59220	AT2G25510	
	AT1G03400	AT4G36850	
	AT2G39710	AT3G14440	
	AT2G37760	AT4G36740	
	AT2G46440	AT1G62940	
	AT2G24850	AT3G18550	
	AT2G31083		

Supplemental Table 6. Differential-expressed genes regulated by BRC1

Up-regulated genes in *brc1* (VS Col-0)	Down-regulated genes in *brc1* (VS Col-0)
AT1G62180	AT2G14560
AT1G04770	AT3G57260
AT5G15120	AT2G18550
AT4G08950	AT3G20810
AT3G02550	AT4G36740
AT3G03270	AT5G60900
AT1G05680	AT3G14620
AT1G58370	AT1G72910
AT1G72430	AT4G14400
AT5G64120	AT3G12220
AT3G27220	AT5G10760
AT4G25100	AT2G24850
AT5G39580	AT2G25510
AT2G38240	AT3G14440
AT4G24110	AT5G52760
AT3G20395	AT2G40080
AT2G19800	AT3G48650
AT2G02990	AT2G46430
AT5G39890	AT1G52100
AT3G10040	AT3G19710
AT2G16060	AT3G23120
AT4G10265	AT3G25620
AT1G43800	AT2G32160
AT4G33560	AT5G42900
AT4G33070	AT1G21250
AT4G39675	AT1G16410
	AT3G50470
	AT1G35710
	AT3G60420
	AT5G66700
	AT4G02280
	AT5G64110
	AT1G73805
	AT4G14365
	AT2G47130
	AT5G24210
	AT4G23170
	AT2G46440
	AT3G26210
	AT3G50480
	AT2G43570
	AT4G33980
	AT5G42530
	AT1G31580
	AT3G19200
	AT1G45145
	AT1G69490
	AT5G57340
	AT3G09260
	AT2G46680
	AT4G22505
	AT5G24530
	AT5G17760
	AT5G59670
	AT2G14610
	AT2G47770
	AT3G17520
	AT5G16920

Supplemental Table 7. Primers for genotyping, CHIP, EMSA, qPCR and recombinant vectors.

Name	sequences 5'-3'
smxl6-LP	AGCCAGAGAAAGACTCGAACC
smxl6-RP	TCAGATCCGAATCGTGAGTTC
smxl7-LP	CGTATTAGCCTCTCGGATTCC
smxl7-RP	GATCAAGAAACGAACGCTGAG
smxl8-LP	TAGCGAAACAATGCTTAACGG
smxl8-RP	TGGTGAGTAACTGCAAATCCC
max2-1-LP	TACATGCAAGCATGCAACTTC
max2-1-RP	AATAGGAACAAAATCGCCACC
LBP1.3	ATTTTGCCGATTTCGGAAC
ChIP-*BRC1*pro-F1-F	ACGTAAGAAAAAGGAGCTACCC
ChIP-*BRC1*pro-F1-R	CATCAATCATGGCGATCCCTC
ChIP-BRC1pro-F2-F	CTTGAGGGATCGCCATGATTG
ChIP-BRC1pro-F2-R	TGATTTGCATTTCACCGTAAG
ChIP-BRC1pro-F3-F	TGACCTTAGTTCTTTCTTACGGTGA
ChIP-BRC1pro-F3-R	AGCATGCACTAAAAGATGCCTAAA
ChIP-BRC1pro-F4-F	TTTAGGCATCTTTTAGTGCATGCT
ChIP-BRC1pro-F4-R	ACAACACAGGCGACGTACTT
ChIP-BRC1pro-F5-F	AAGTACGTCGCCTGTGTTGT
ChIP-BRC1pro-F5-R	TGTTCATGCCTTTTTAGGGGT
BRC1-pro-probe a-F	GAACAAATGCAATATATCAATAGTTAGTGTACATATGAAG
BRC1-pro-probe a-R	CTTCATATGTACACTAACTATTGATATATTGCATTTGTTC
BRC1-pro-probe b-F	AACATAAACAAACACAAGGTCCTAATTATAGAAAAAAATC
BRC1-pro-probe b-R	GATTTTTTTCTATAATTAGGACCTTGTGTTTGTTTATGTT
BRC1-pro-probe c-F	AAGAAGATTATAGTACAAGTGTCATTCTCAAAATTTTGTC
BRC1-pro-probe c-R	GACAAAATTTTGAGAATGACACTTGTACTATAATCTTCTT
BRC1-qPCR-F	GGAAACAAGGTCGATGGGAGA
BRC1-qPCR-R	TTTAAAATGGGCGTTCGCGG
BES1-qPCR-F	GGCTACTATACCTGAATGTG
BES1-qPCR-R	AGAGAATGGCTGTTGTTG
U-BOX-F	TCTTCTTCTGCTACATCTACTCTC
U-BOX-R	AGTGTGTGAACCCGTGAAC
ACT2-F	TGCTGTTGACTACGAGCAGG
ACT2-R	TCCATTCCCACAAACGAGGG
ChIP-*DWF4*pro-F	GACAATGCCAAAAGTCTACGGG
ChIP-*DWF4*pro-R	GGAGCTAGTTTCTCTCTCTCTC
BES1-F	ATGACGTCTGACGGAGCAAC
BES1-R	ACTATGAGCTTTACCATTTCC
BES1-L-F	ATGAAAAGATTCTTCTATAATTCCAGC
BES1pro -F	ATATTAGTATCACTATTCTGCTATTCACTAG
Overlapping-bes1-D-F	CCTGGCTACTAT ACCTG
Overlapping-bes1-D-R	CAGGTATAGTAGCCAGG

SMXL6-F	ATGCCGACGCCGGTGACTACGG
SMXL6-R	CCATATCACATCCACC
SMXL7-F	ATGCCGACACCAGTAACC
SMXL7-R	GATCACTTCGACTCTC
SMXL8-F	ATGCCAACGGCGGTGAAT
SMXL8-R	CTACTGAGATTTTACAAA
*SMXL7*pro-F	TCTACTGTGCATCAAGACAT
overlapping-*SMXL7*-D-F2	CAGATTGTCTGAGGCTATGACACTCCGTGACTCGCATGGG
overlapping-*SMXL7*-D-R2	CCCATGCGAGTCACGGAGTGTCATAGCCTCAGACAATCTG
overlapping-*SMXL7*-mEAR-F2	GCGTTCGTTTGCTGATGCAAATGCTCCTGTGGATGAG
Overlapping-*SMXL7*-mEAR-F2	GCGTTCGTTTGCTGATGCAAATGCTCCTGTGGATGAG